2009

Tracking in Wireless Sensor Network Using Blind Source Separation Algorithms

Anil Babu Vikram
Cleveland State University

TRACKING IN WIRELESS SENSOR NETWORK USING BLIND SOURCE SEPARATION ALGORITHMS

ANIL BABU VIKRAM

Bachelor of Technology (B.Tech)

Electronics and Communication Engineering(E.C.E)

Jawaharlal Nehru Technological University,India

May, 2006

submitted in partial fulfillment of the requirements for the degree

MASTER OF SCIENCE IN ELECTRICAL ENGINEERING

at the

CLEVELAND STATE UNIVERSITY

NOVEMBER, 2009

This thesis has been approved for the

Department of **ELECTRICAL AND COMPUTER ENGINEERING**

and the College of Graduate Studies by

Thesis Committee Chairperson, Dr. Ye Zhu

Department/Date

Dr. Vijay K. Konangi

Department/Date

Dr. Yongjian Fu

Department/Date

To my Parents and Friends

ACKNOWLEDGMENTS

I would like to thank my advisor Dr.Ye Zhu, for constant support, motivation and guidance.

I would like thank committee members Dr. Vijay K. Konangi, Dr. Yongjian Fu for their support. I am very appreciate for Dr. Zhu giving me an opportunity to work in Network Security and Privacy research group.

I would like to thank my research group members for their support and friendship.

Special thanks and appreciation go to my family and friends for their moral and physical support. Special thanks to my sister Sakuntala and a good friend Srikar for constant moral support.

TRACKING IN WIRELESS SENSOR NETWORK USING BLIND SOURCE SEPARATION ALGORITHMS

ANIL BABU VIKRAM

ABSTRACT

This thesis describes an approach to track multiple targets using wireless sensor networks. In most of previously proposed approaches, tracking algorithms have access to the signal from *individual* target for tracking by assuming (a) there is only one target in a field, (b) signals from different targets can be differentiated, or (c) interference caused by signals from other targets is negligible because of attenuation. We propose a general tracking approach based on *blind source separation*, a statistical signal processing technique widely used to recover individual signals from mixtures of signals. By applying blind source separation algorithms to *mixture* signals collected from sensors, signals from *individual* targets can be recovered. By correlating *individual* signals recovered from different sensors, the proposed approach can estimate paths taken by multiple targets. Our approach fully utilizes both temporal information and spatial information available for tracking. We evaluate the proposed approach through extensive experiments. Experiment results show that the proposed approach can track multiple objects both accurately and precisely. We also propose cluster topologies to improve tracking performance in low-density sensor networks. Parameter selection guidelines for the proposed topologies are given in this Thesis. We evaluate proposed cluster topologies with extensive experiments. Our empirical experiments also show that BSS-based tracking algorithm can achieve comparable tracking performance in comparison with algorithms assuming access to *individual signals*.

TABLE OF CONTENTS

LIST OF TABLES

LIST OF FIGURES

List of Algorithms

CHAPTER I

INTRODUCTION

Tracking moving targets with wireless sensors is one of the prominent applications of wireless sensor networks. Sensors, also called as "smart dust" [47], are small devices known for their simplicity and low cost. Using a network of sensors with wireless communication capability enables both cost-effective and performance-effective approaches to track targets, due to the availability of large amount of data collected by sensors for tracking targets. Depending on the applications, sensors with different sensing modalities such as acoustic, seismic, infrared, radio, and magnetic can be deployed for tracking different type of targets.

In general, data collected by sensors is *aggregate* data. In the signal processing language, signals received by sensors are generally *mixtures* of signals from *individual* targets. For example, an acoustic sensor in a field of interest may receive sound signals from more than one target. Obviously tracking targets based on mixture signals can result in inaccurate results when interference from targets other than the one of interest is not negligible. For brevity, we use the term *aggregate signal* to mean the signal received by sensor, i.e., data collected by sensors and *individual signal* to mean the signal transmitted from or caused by individual targets in the rest of the

Thesis.

The fact that signals collected by sensor networks are aggregate signals, poses a big challenge to target-tracking solutions. The problem space of the target-tracking problem is divided and special cases of the target-tracking problem have been well studied:

- Single-target case: In this case, it is assumed that only one target exists in a field of interest. So signals received by sensors are essentially *individual signals*.
- Negligible interference case: Some researches assume that interference from targets other than the one of interest is negligible. The assumption is legitimate only for applications in which signal from a target attenuates dramatically when distance between the target and sensor increases.
- Distinguishable target case: Sensors can distinguish targets by tags embedded in signals or by having different targets to send signals using different channels such as using different frequency bands.

All these special cases assume that tracking algorithms can have access to individual signals. Singh et al. [52] proposed a general approach to track multiple targets indistinguishable by sensors. The approach is based on binary proximity sensors that can only report whether or not there are targets in sensing areas. The approach is simple and robust to interference from other targets with the cost of the limitation that it is only applicable to track targets in smooth paths [52].

We propose an approach based on Blind Source Separation, a methodology from statistical signal processing to recover unobserved "source" signals from a set of observed mixtures of the signals. Blind source separation models were originally defined to solve the *cocktail party problem*: The blind source separation algorithms can extract one person's voice signal from given mixtures of voices in a cocktail party.

Blind source separation algorithms solve the problem based on the independence between voices from different persons. Similarly, in the target-tracking problem, it is generally safe to assume *individual signals* from different targets are independent. So, we can use blind source separation algorithms to recover *individual signals* from *aggregate signals* collected by sensors. For the cases in which *individual signals* are dependent, blind source separation algorithms based on timing structure [56] of *individual signals* can be used.

The proposed algorithm utilizes both temporal information and spatial information available to track targets. Applying blind source separation algorithms on aggregate signals collected by sensors can recover *individual signals*. But the output of blind source separation algorithms includes not only recovered individual signals, but also noise signals, aggregate signals and partial signals, which contain part of individual signals in different time durations. Clustering is used in our algorithm to pick out the individual signals from signal output by the blind source separation algorithms. A voting step based on spatial information is used to further improve the performance of the algorithm.

The contributions of this Thesis can be summarized as follows:

- We proposed a general approach to track multiple targets in a field. The approach can be applied in real-world applications where targets are indistinguishable and interference from targets other than the one of interest is not negligible.

- We evaluate our approach with both empirical experiments and simulations. We also analyze the effect of parameters used in the proposed approach experimentally and theoretically.

- We propose metrics to evaluate performance of target-tracking algorithms. The metrics originate from the general metrics used to evaluate performance of an

estimator in statistics since, essentially, target tracking algorithms *estimate* the paths based on data collected from sensor networks.

- According to our knowledge, we are the first to apply blind source separation to process data collected from wireless sensor networks. Blind source separation algorithms are useful tools for processing data collected from wireless sensor networks since, essentially, data collected from sensors are all *aggregate* data. In this Thesis we focus on applying blind source separation in the target-tracking problem. The blind source separation algorithms can also be used to process data in other applications of wireless sensor networks such as location detection and factor analysis. For most applications of wireless sensor networks, analysis based on *individual* signals can yield more accurate results.

1.1 Organization of the Thesis

The rest of the thesis is organized as follows: In Chapter 2, we review related work. Chapter 3 outlines our network model and assumptions. The main idea of applying blind source separation algorithms in tracking targets is described in Chapter 4. In Chapter 5, we describe our approach in details. We theoretically analyzed the performance of our approach and effect of parameters used in our approaches in Chapter6. The evaluation of our approach by empirical experiments and simulations is presented in Chapter 7 and Chapter 8 respectively. In Chapter 9 we discuss on topologies of sensor network to improve tracking performance and formally defines the problem in randomly placed low-density networks. We describe proposed topologies in Chapter 10. We evaluate proposed topologies under various settings in Chapter 11. We discuss possible extension to our approach and outline our future work in Chapter 12. The thesis concludes in Chapter 13.

CHAPTER II

RELATED WORK

Multiple-target tracking originates from military applications such as tracking missiles and airplanes with radars and tracking vessels with sonars [53]. In these applications, sensors such as radars and sonars are able to scan a field of interest with beams operating in selected resolution modes and in selected beam directions. The tracking systems track targets based on deflection from targets. Algorithms based on particle filtering and kalman filtering were proposed for these applications [18, 31, 40, 57, 58]. In this Thesis, we assume simple wireless sensors, which can only report signal strength and has no capability to determine signal directions, are used for target tracking.

Wireless sensors, known for their simplicity and low cost, have been proposed or deployed to track targets in various applications. The examples are tracking robots with infrared signals [9], tracking vehicles with infrared signals [20], tracking ground moving targets with seismic signals [43], tracking moving vehicles with acoustic sensors [26], and tracking people with RF signals [45]. Location detection, equivalent to tracking static targets, has also been studied extensively. This topic has been investigated in different wireless networks such as wireless sensor networks [49, 50], wireless

LANs [2], and wireless ad-hoc networks [12, 61].

Most approaches proposed to track targets or detect location are based on characteristics of physical signals such as angle of arrival (AOA) [14, 36, 39], Time of Arrival (TOA) [37,41], Time Difference of Arrival (TDOA) [11,48] and Received Signal Strength (RSS) [25, 62]. Receiver signal strength is widely used in tracking targets with wireless sensor networks [2,34]. Most of the previous researches focus on tracking a single target [1, 16, 29, 42, 51] or assume targets are distinguishable [20, 35, 38, 60].

A string of researches on tracking targets with wireless sensor networks are based on binary proximity sensors which can only report whether there are targets within sensing areas. The initial work [1, 29, 51] on binary proximity sensors focuses on tracking single target. Singh et al. [52] extended the approach to track multiple indistinguishable targets by applying particle filtering algorithms. Approaches based on binary proximity sensors have two obvious advantages: (a) The sensors are very simple since they only report binary information. (b) The approaches are robust since interference from other targets are essentially filtered out by an equivalent low-pass filter [51]. The cost of using these simple devices is loss of information that is helpful to accurately track targets due to the filtering effect. So, approaches based on binary proximity sensors can not track target in a path with high-frequency variations [51]. We propose a general approach to track multiple indistinguishable targets. The approach is based on blind source separation algorithms, which can recover individual signals from aggregate signals. So, the challenging problem of tracking multiple targets becomes a much easier problem, equivalent to tracking single targets. Since individual signals can be fully recovered, our approach can track targets following paths with high-frequency variations.

CHAPTER III

NETWORK MODEL AND ASSUMPTIONS

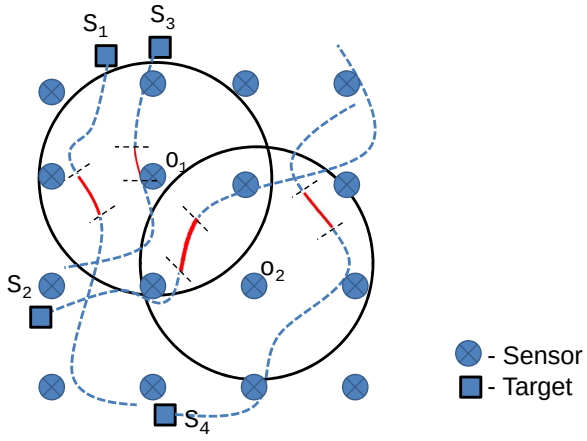

Figure 1: Network Model. In the figure, the dashed lines represent the targets moving paths and the red stripes in the moving paths represent path segments that targets are moving on simultaneously. The solid circles represent sensing ranges of Sensors O_1 and O_2.

A general model of tracking targets using wireless sensor networks is shown in Figure 1. Wireless sensors are randomly deployed in the field of interest. Generally, a wireless sensor can receive a mixture of individual signals from multiple sources. For example, suppose acoustic sensors are deployed in Figure 1, Sensor O_1 can receive audio signals from Targets S_1, S_2, and S_3 during one time duration. Following are

the assumptions made in this general model:

- Sensors have no capability to distinguish targets. This assumption is important for deploying sensors in uncooperative or hostile environments such as tracking enemy soldiers with wireless sensor networks.

- The location of each sensor in the sensor network is known. Location information can be gathered in a variety of ways. For example, the sensors may be planted, and their location is marked. Alternatively, sensors may have GPS capabilities. Finally, sensors may locate themselves through one of several schemes that rely on sparsely located anchor sensor nodes [6].

- Aggregate signals collected by wireless sensors can be gathered for processing by a sink or gateway. Data compression or coding schemes designed for sensor networks such as ESPIHT [54,59] can be used to reduce the data volume that is caused by remaining spatial redundancy across neighboring nodes or temporal redundancy at individual nodes.

- Targets are moving under a speed limit. Obviously it is impossible to track a high-speed target that only generates a small amount of data when passing the field of interest. We analyze the effect of the speed limit in Chapter 6.

CHAPTER IV

APPLICATION OF BLIND SOURCE SEPARATION ALGORITHMS IN TRACKING TARGET

In this Chapter, we introduce blind source separation and the rationale of applying blind source separation to the multiple target tracking problem using wireless sensor networks.

4.1 Blind Source Separation

Blind Source Separation (BSS) is a methodology used in statistical signal processing to recover unobserved "source" signals from a set of observed mixtures of the signals. The separation is called *blind* to emphasize that the source signals are not observed and that the mixture is a black box to the observer. While no knowledge is available about the mixture, in many cases it can be safely assumed that source signals are independent. In its simplest form [7] , the blind source separation model assumes n independent signals $S_1(t), \cdots, S_n(t)$ and n observations of mixture $O_1(t), \cdots, O_n(t)$ where $O_i(t) = \sum_{j=1}^{n} a_{ij} S_j(t)$. The goal of BSS is to reconstruct the source signals $S_j(t)$ using only the observed data $O_i(t)$, the assumption of independence among the

signals $S_j(t)$. Given the observations $O_i(t)$, BSS techniques estimate the signals $S_j(t)$ by maximizing the independence between the estimated signals. A very nice introduction to the statistical principles behind BSS is given in [7]. The common methods employed in blind source separation are minimization of mutual information [8, 23], maximization of nongaussianity [27], and maximization of likelihood [17,46]. Timing-structure based algorithms [55, 56] can be used to recover source signals when source signals are dependent.

4.2 Recover *Individual Signals* for Target-Tracking with Blind Source Separation Algorithms

In our tracking approach, blind source separation algorithms are used to recover *individual signals* (i.e., source signals as in the BSS literature introduced in Chapter 4.1) from *aggregate signals* (i.e., observations as in the BSS literature introduced in Chapter 4.1). Suppose acoustic sensors are deployed in the field shown in Figure 1, Sensor O_1 can receive audio signals from Targets S_1, S_2, and S_3 and Sensor O_2 can receive audio signals from Targets S_2 and S_4. If we represent the signal received by Sensor O_i as $O_i(t)$ and the individual signal from Target S_i as $S_i(t)$, we can have following two equations: $O_1(t) = S_1(t) + S_2(t) + S_3(t)$, $O_2(t) = S_2(t) + S_4(t)$. In general, for m neighboring sensors and n targets, we can rewrite the problem in vector-matrix notation,

$$\begin{pmatrix} O_1(t) \\ O_2(t) \\ \vdots \\ O_m(t) \end{pmatrix} = \mathbf{A}_{m\times n} \begin{pmatrix} S_1(t) \\ S_2(t) \\ \vdots \\ S_n(t) \end{pmatrix} \tag{4.1}$$

where $\mathbf{A}_{m\times n}$ is called *mixing matrix* in the BSS literature. Since the individual signals are independent from each other - they come from different targets - we can use any of the algorithms mentioned in Chapter 4.1 to recover individual signals $S_1(t), \cdots, S_n(t)$.

While the goal of BSS in this context is to re-construct the original signals $S_i(t)$, in practice the separated signals are sometimes only loosely related to the original signals. We categorize these separated signals into four types, as follows: In the first case, the separated signal is correlated to actual individual signals $S_i(t)$. The separated signal in this case may have a different sign than the original signal. We call this type of separated signal an *individual separated signal*. In the second case, a separated signal may be correlated to an *aggregate of signals* from several targets. This happens when signals from more than two targets can be "heard" by all the sensors. In such a case, the BSS algorithm would not be able to fully separate the signal mixture into the individual separated signals. Rather, while some individual signals can be successfully separated, others remain aggregated. In the third case, separated signals may be correlated to one original signal in the beginning part and correlated to another original signal in the rest. We call this type of separated signal a *partial separated signal*. This happens when a target moves out of one sensing range and enters into another sensing range. In the fourth case, separated signals may represent *noise signals*.

Noise signals are separated out when neighboring sensors receive different individual signals from the same target. The difference can be caused by signal attenuation or environment noise. BSS algorithms separate the difference as noise signals. The effect of signal attenuation on separation performance is described in Chapter 6.1.

CHAPTER V

TRACKING ALGORITHM

The tracking algorithm consists of six steps: (1) Aggregate signals collected from sensors are grouped and segmented and these groups of signal segments are fed to the second step, the blind source separation step. (2) The blind source separation step outputs separated signals. As described in Chapter 4, these separated signals contain individual separated signals, aggregate separated signals, noise signals, and partial separated signals. (3) The clustering step will cluster these separated signals. (4) The center selection step selects separated signals that are closest to actual individual signals from clusters formed in the clustering step. (5) The intersection step estimates segments of paths based on separated signals selected from the previous step. (6) The voting step outputs estimated paths by voting on path segments generated in the intersection step. The details of these six steps (preparation, separation, clustering, center selection, intersection, voting) are described below.

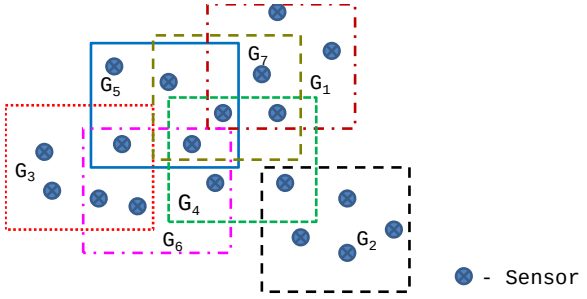

Figure 2: Grouping ($n_{group} = 5$). In the figure, sensors within a rectangular form a sensor group.

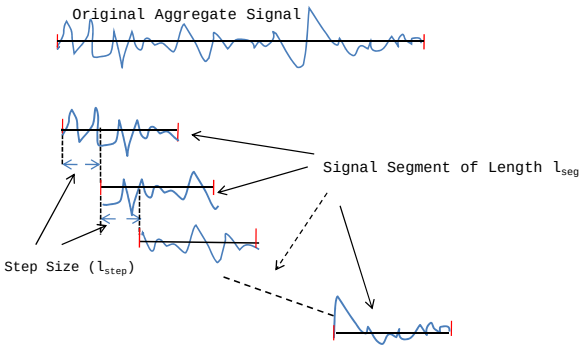

Figure 3: Signal Segments

5.1 Preparation Step

To fully utilize information collected from wireless sensor networks, aggregate signals collected by wireless sensors are grouped spatially and segmented temporally. As shown in Figure 2, sensors in the field are grouped into sensor groups. Each group has n_{group} neighboring sensors. We use N_{grps} to denote the total number of sensor groups formed. Aggregate signals collected from each sensor group are segmented according to time slots shown in Figure 3. Time slots are of length l_{seg}. The step size between two successive time slots is l_{step}. So two successive signal segments have a common part of length $l_{seg} - l_{step}$. A BSS algorithm will be applied on grouped aggregate signals sequentially, i.e., segment by segment in the next step.

We represent the segment group from the ith sensor group and the jth time slot as $OG_{i,j}$. The pth segment in the group is denoted as $O^p_{i,j}$. In set theory notation, $OG_{i,j} = \{O^p_{i,j} : p = 1, \cdots, n_{group}\}$. The output of the preparation step is segment groups $OG_{i,j}$.

Spatial redundancy and temporal redundancy are created during grouping and segmenting respectively. We use the term, spatial redundancy, to mean the fact that a sensor can be grouped into more than one sensor groups. The temporal redundancy is created in segmenting since two successive time slots have overlap. Both spatial redundancy and temporal redundancy are created to make the tracking algorithm robust against noise and artifacts possibly generated in the following separation step.

After the preparation step, signals are all in unit of segments. We use actual segments, individual segments, aggregate segments, partial segments, noise segments to mean segments of original individual signals, individual separated signals, aggregate separated signals, partial separated signals, and noise signals respectively in the rest of the Thesis.

5.2 Separation Step

In the separation step, a BSS algorithm is applied on segments contained in $OG_{i,j}$ for all i and j. The outputs of the separation step are groups of separated segments denoted by $SG_{i,j}$, i.e., the group of segments separated from $OG_{i,j}$.

5.3 Clustering Step

The clustering step is designed to eliminate noise segments, aggregate segments, and partial segments by taking advantage of spatial redundancy created in the preparation step. The heuristic behind this step is as follows: if a separated signal represents an individual signal, similar signals will be separated in at least similar forms by more than one neighboring sensor groups. In contrast, a separated signal that was generated because of attenuation or interference is unlikely to be generated by more than one group[1]. In our experiments, agglomerative hierarchical clustering [13] is used.

Based on the heuristic, we use correlation as the measure of similarity, and define the distance between two separated segments as follows:

$$D(S'^{p}_{i,j}, S'^{q}_{k,j}) = 1 - |corr(S'^{p}_{i,j}, S'^{q}_{k,j})| \quad , \tag{5.1}$$

where $S'^{p}_{i,j}$ denotes the pth segment in separated segment group $SG_{i,j}$, and $corr(x, y)$ denotes the correlation coefficient of segments x and y. We use the absolute value of the correlation coefficient because the separated segments may be of different sign than the actual segment. Clustering will only cluster segments of the same time slots as indicated in the distance measure defined in Equation 5.1. The number of clusters formed in this step is heuristically set to two times the number[2] of targets in the field

[1] More analysis of attenuation and interference can be found in Chapter 6

[2] The number of targets can be either known *a priori* or can be estimated using existing algorithms

because some clusters may contain only partial segments and noise segments. These clusters of partial segments and noise segments are removed in the following center selection step.

The highly-correlated (similar) segments will cluster together. Figure 5 uses a two-dimensional representation to further illustrate the rationale for the clustering approach in this step. In Figure 5, the two-dimensional representation is only for visualization: Each dot in the figure represents a separated segment of length l_{seg}. For better visualization, we simplify the visualization to be two-dimension. Since it is impossible to draw in a space with more than three dimensions. As shown in this Figure 5, the individual segments form clusters. The aggregate segments and partial segments, on the other hand, scatter in-between these clusters. The noise segments are distant both from each other and from the other segments.

In summary, the input of the clustering step is $SG_{i,j}$ and the clustering step outputs clusters formed in each time slots. We use $Clst_j^i$ to denote the ith cluster formed in the jth time slot.

5.4 Center Selection Step

The goal of the center selection step is to select center segments as shown in Figure 5 from clusters formed in the previous step. Center segments are the segments in the center of each cluster formed according to the distance measure as defined in Equation 5.1.

The center selection step is based on the temporal redundancy created in the preparation step. For ease of understanding, we use the example in Figure 4 to describe the rationale behind the center selection step. Because of the overlap between

[3, 5, 15]. Similar tracking performance was observed with more clusters mainly because of the following center selection step.

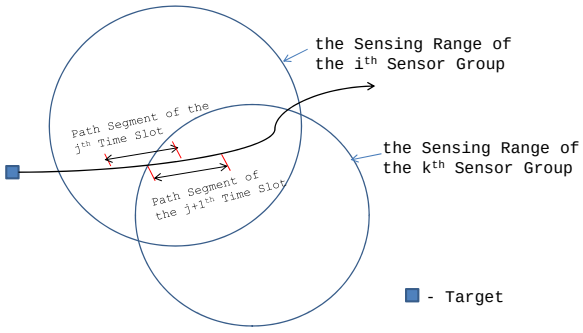

Figure 4: Rationale Behind The Center Selection Step

the sensing range of the ith sensor group and the sensing range of the kth sensor group, both sensor groups are are able to "hear" the target at the same time. Without loss of generality, we assume both sensor groups can "hear" the target from the $j+1$th time slot. Because of the temporal redundancy as described in Chapter 5.1, the $j+1$th time slot has a common part of length $l_{seg} - l_{step}$ with the jth time slot. In turn, the signal received from the target by the ith sensor group during the jth time slot has a *common* part with the signal received from the same target by the kth sensor group during the $j+1$th time slot. So one of the separated segment from the ith sensor group and jth time slot, denoted as[3] $S'^{p}_{i,j}$, should be similar as one separated segment from the kth sensor group and $j+1$th time slot, denoted as $S'^{q}_{k,j+1}$. To measure the similarity, we define the link correlation between the two separated segments as follows:

$$\rho(S'^{p}_{i,j}, S'^{q}_{k,j+1}) = |corr(S'^{p}_{i,j}(l_{step}, l_{seg}), S'^{q}_{k,j+1}(0, l_{seg} - l_{step}))| \quad , \tag{5.2}$$

where $S'^{p}_{i,j}(x,y)$ denotes the part of Segment $S'^{p}_{i,j}$ from the xth data sample to the yth data sample and $\rho(S'^{p}_{i,j}, S'^{q}_{k,j+1})$ denotes the link correlation between segments $S'^{p}_{i,j}$ and $S'^{q}_{k,j+1}$. Absolute value is used in link correlation definition because the separated

[3]To differentiate separated signals from original individual signals, we use S' to denote separated signals and S to denote original individual signals.

segments may be of different sign than the actual segments.

The example in Figure 4 shows the case when a target is moving along a path. If the target is static within the sensing range of the ith sensor group, then the link correlation $\rho(S_{i,j}^{'p}, S_{i,j+1}^{'q})$ should be high. In other words, one separated segment from the ith sensor group and the jth time slot, denoted as $S_{i,j}^{'p}$, should be very similar as one of the separated segment from the same sensor group and the $j+1$th time slot, denoted as $S_{i,j+1}^{'q}$. To generalize the two cases, we redefine the link correlation as follows:

$$\rho(S_j^{'p}, S_{j+1}^{'q}) = |corr(S_j^{'p}(l_{step}, l_{seg}), S_{j+1}^{'q}(0, l_{seg} - l_{step}))| \quad , \tag{5.3}$$

where $S_j^{'p}$ denotes the pth separated segment from the jth time slot among segments separated from all sensor groups[4].

The center selection step can prevent centers of noise-segment clusters and partial-segment clusters from being selected since noise and artifact generated by separation algorithms in one time slot will unlikely be generated again in the following time slot. To make the algorithm more robust, we design the algorithm to calculate the link correlation for n_{slot} consecutive time slot (CTS), i.e.,

$$\mathrm{P}_{CTS_j}(S_j^{'x_j}, S_{j+1}^{'x_{j+1}}, \cdots, S_{j+n_{slot}}^{'x_{j+n_{slot}}}) = \sum_{i=j}^{j+n_{slot}-1} \rho(S_i^{'x_i}, S_{i+1}^{'x_{i+1}}) \quad , \tag{5.4}$$

we use CTS_u to denote uth CTS containing time slots $\{u, u+1, \cdots, u+n_{slot}-1\}$. In each time slot, the K center segments with top K sum of link correlation defined in Equation 5.4 are selected. Only one center segment will be selected from a cluster. The number of center segments selected in each time slot is K, the number of targets in the field. The value of K is either known *a priori* or can be estimated by using existing algorithms [3, 5, 15].

[4]We remove i the index of sensor groups, from $S_{i,j}^{'p}$, since link correlation can be calculated for different sensor groups and the same sensor group. In the rest of the Thesis, we use $S_j^{'p}$ to denote the pth segment separated from the jth time slot among segments separated from all sensor groups.

The pseudo code of the center selection step is shown in Algorithm 1. The input to the center selection step is $Clst_j^i$ and the output is center segments $C_{k,j}^u$ that denotes the kth center segment selected for jth time slot based on CTS_u.

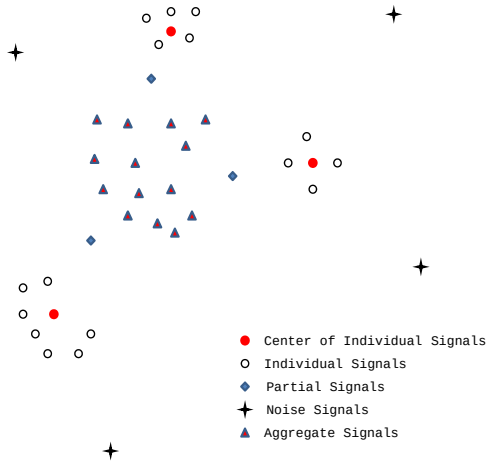

Figure 5: Clustering

5.5 Intersection Step

The intersection step estimates one segment of a path based on each center segment selected in the previous step. One path segment is estimated by geographically intersecting the sensing ranges of sensor groups that can "hear" the same target. Since center segments are segments most "resembling" to the original individual segments from targets, the sensor groups which can "hear" the same target can be found as follows: For one center segment $C_{k,j}^u$ (denoting the kth center segment selected for the jth time slot based on CTS_u), if a sensor group has one separated segment $S_j^{\prime m}$ (denoting the mth separated segment among all the segments separated in the jth time slot) highly correlated to the center segment $C_{k,j}^u$, the sensor group is determined as a sensor group which can "hear" a target.

The order of sensing ranges being intersected is determined by the absolute

input : v - number of time slots available for tracking, K - number of center segments in each time slot, Clusters formed in the previous clustering step ($Clst_j^i$, denoting the ith cluster formed in the jth time slot), Separated Segments ($S_j^{\prime m}$, denoting the mth separated segments among all the segments separated in jth time slot);

output: Selected center segments ($C_{k,j}^u$, denoting the kth center segment selected for jth time slot based on CTS_u);

Initialize $C_{k,j}^u = 0$ for all k, j, and u;
for $j \leftarrow 1$ **to** $v - n_{slot} + 1$ **do**
    Initialize $ClstLabel_{i,j} = 0$ for all i and j; `/* ` $ClstLabel_{i,j}$ `denotes the label for the` i`th cluster in` j`th time slot */`;
    foreach *combination of separated segments* $(S_j^{\prime x_j}, S_{j+1}^{\prime x_{j+1}}, \cdots, S_{j+n_{slot}}^{\prime x_{j+n_{slot}}})$ **do**
        Calculate sum of link correlation $\mathrm{P}_{CTS_j}(S_j^{\prime x_j}, S_{j+1}^{\prime x_{j+1}}, \cdots, S_{j+n_{slot}}^{\prime x_{j+n_{slot}}}) = \sum_{i=j}^{j+n_{slot}-1} \rho(S_i^{\prime x_i}, S_{i+1}^{\prime x_{i+1}})$;
    end
    sort P_{CTS_j} in descending order;
    for $k \leftarrow 1$ **to** K **do**
        while $C_{k,j}^j == 0$ **do**
            Pick the largest sum of link correlation $\mathrm{P}_{CTS_j}(S_j^{\prime y_j}, S_{j+1}^{\prime y_{j+1}}, \cdots, S_{j+n_{slot}}^{\prime y_{j+n_{slot}}})$ from the set of P_{CTS_j};
            remove $\mathrm{P}_{CTS_j}(S_j^{\prime y_j}, S_{j+1}^{\prime y_{j+1}}, \cdots, S_{j+n_{slot}}^{\prime y_{j+n_{slot}}})$ from the set of P_{CTS_j};
            for $i \leftarrow j$ **to** $j + n_{slot}$ **do**
                find $ClstLabel_{z_i,i}$ so that $S_i^{\prime y_j} \in Clst_{z_i,i}$;
            end
            if $ClstLabel_{z_i,i} == 0$ *for all* i *between* j *and* $j + n_{slot}$ **then**
                for $i \leftarrow j$ **to** $j + n_{slot}$ **do**
                    $ClstLabel_{z_i,i} = 1$;
                    $C_{k,i}^j = S_i^{\prime z_i}$;
                end
            end
        end
    end
end

Algorithm 1: Center Selection Step

value of the correlation. Absolute values are used because the individual segments may be of different signs than the actual segments. In other words, the sensor groups are first ordered based on the absolute value of the correlation with the center segment $C^u_{k,j}$. The two sensor groups having top two absolute correlation values will have their sensing ranges intersected first. The resulting intersection area will be intersected again with the sensing range of the sensor group having the next highest absolute value of correlation with the center segment. The intersection stops when the intersection area is empty. The estimated path segment is the intersection area obtained before the last intersection.

The input of this step is center segments $C^u_{k,j}$. For each center segment, an intersection area $area^u_{k,j}$ is generated as output of this step. These generated areas are estimated path segments. The pseudo code for the intersection step can be found in Algorithm 2.

5.6 Voting Step

The voting step concatenates the "best" path segments estimated in the previous step to form an estimated path. The "best" path segments are selected by a voting mechanism. Before explaining the details of the voting mechanism, we would like to first introduce the distance metric d_{area} which measures the distance between two estimated path segments, i.e., two intersection areas output by the intersection step. The distance $d_{area}(area^u_{X,j}, area^u_{Y,j+1})$, i.e., the distance between two path segments denoted by $area^u_{X,j}$ and $area^u_{Y,j+1}$, is defined as the minimum distance between any two points from these two path segments respectively. So if the two path segments overlap with each other, then $d_{area}(area^u_{X,j}, area^u_{Y,j+1}) = 0$.

The voting mechanism takes advantage of the temporal redundancy created in the preparation step. The "best" path segment selected to form an estimated path

input : n_{group} - number of sensors per group, K - number of center segments in each time slot, Selected center segments ($C^u_{k,j}$, denoting the kth center segment selected for the jth time slot based on CTS_u), Separated Segments (S'^m_j, denoting the mth separated segments among all the segments separated in the jth time slot)

output: Intersection areas ($area^u_{k,j}$, denotes the kth intersection area for the jth time slot based on CTS_u)

1 **for** $k \leftarrow 1$ **to** K **do**
2 **for** $j \leftarrow 1$ **to** $v - n_{slot} + 1$ **do**
3 **for** $u \leftarrow j$ **to** $j + n_{slot} - 1$ **do**
4 **foreach** *separated segment* S'^m_j **do**
5 $Corr^u_{k,j}(m) = corr(S'^m_j, C^u_{k,j})$;
6 **end**
7 sort the array $Corr^u_{k,j}$ in descending order;
8 set tmp_{area} to cover the whole field;
9 **while** tmp_{area} ! $= NULL$ **do**
 /* $NULL$ means empty */
10 select the current largest absolute correlation from the array $Corr^u_{k,j}$ and find corresponding separated segment S'^m_j (without loss of generality, suppose S'^m_j is separated from the lth sensor group);
11 remove the current largest absolute correlation from the array $Corr^u_{k,j}$;
12 $area^u_{k,j} = tmp_{area}$;
13 $tmp_{area} = tmp_{area} \cap$ the sensing range of the lth sensor group;
14 **end**
15 **end**
16 **end**
17 **end**

Algorithm 2: Intersection Step

should satisfy the following two requirements: (1) The selected path segment $area^u_{k,u}$ should have zero distance with all path segments estimated based on the same CTS_u, i.e., $dcur_{k,u} = \sum_{j=u}^{u+n_{slot}-2} d_{area}(area^u_{k,u}, area^u_{k,j+1}) = 0$. The selected path segment should also have zero distance with all the path segments estimated for the same time slot based on different CTS, i.e.,

$dpre_{k,u} = \sum min(d_{area}(area^u_{k,u}, area^{u-m}_{1,u}), \cdots, d_{area}(area^u_{k,u}, area^{u-m}_{K,u})) = 0.$

Finally a path is estimated by linking path segments selected from different time slots. To determine whether a selected "best" path segment, say $Pseg_{z_j,j}$ denoting the z_jth selected path segment for the jth time slot, belongs to a path, say $epath_l$ denoting the lth estimated path, the distance between $Pseg_{z_j,j}$ and the path segment of $epath_l$ determined in the previous time slot, say $Pseg_{z_{j-1},j-1}$, is calculated. If the distance is zero, then $Pseg_{z_j,j}$ is determined as one path segment of $epath_l$. The pseudo code of the voting step is shown in Algorithm 3 and Algorithm 4.

input : K - number of estimated segments in each time slot, v - number of time slots available, Estimated path segments ($area^u_{i,j}$ - the ith estimated segment among all the estimated segments in the jth time slot based on CTS_u;
output: $epath_l$ - Estimated path of the lth moving target.

1 **for** $u \leftarrow 1$ **to** $v - n_{slot} + 1$ **do**
2 **for** $k \leftarrow 1$ **to** K **do**
3 $dcur_{k,u} = \sum_{j=u}^{u+n_{slot}-2} d_{area}(area^u_{k,u}, area^u_{k,j+1})$;
  /* $dcur_{k,u}$ is sum of distance between estimated segments in the uth time slot and other time slots estimated in the same CTS_u. */
4 **if** $u > 1$ && $u < n_{slot}$ **then**
  /* Boundary Case */
  $dpre_{k,u} = \sum_{m=1}^{u-1} min(d_{area}(area^u_{k,u}, area^{u-m}_{1,u}),$
  $d_{area}(area^u_{k,u}, area^{u-m}_{2,u}), \cdots,$ /* $dpre_{k,u}$ is
5 $d_{area}(area^u_{k,u}, area^{u-m}_{K,u}))$;
  sum of minimum distance between estimated segments in the uth time slot in current CTS and the uth time slot in all previous CTS. */
6 **else**
  $dpre_{k,u} = \sum_{m=1}^{n_{slot}-1} min(d_{area}(area^u_{k,u}, area^{u-m}_{1,u}),$
  $d_{area}(area^u_{k,u}, area^{u-m}_{2,u}), \cdots,$
7 $d_{area}(area^u_{k,u}, area^{u-m}_{K,u}))$;
8 **end**
9 **if** $dcur_{k,u} == 0$ && $dpre_{k,u} == 0$ **then**
10 $Pseg_{k,u} = area^u_{k,u}$; /* $Pseg_{k,u}$, denote the kth estimated segment in the uth time slot */
11 **else**
12 $Pseg_{k,u} = -1$; /* -1, means not selected */;
13 **end**
14 **if** $u == v - n_{slot} + 1$ **then**
15 **for** $i \leftarrow u$ **to** $v - 1$ **do**
16 **if** $d_{area}(area^u_{k,u}, area^u_{k,i+1}) == 0$ **then**
17 $Pseg_{k,i+1} = area^u_{k,i+1}$;
18 **else**
19 $Pseg_{k,i+1} = -1$;
20 **end**
21 **end**
22 **end**
23 **end**
24 **end**
  /* Continuation of Voting Step is shown in Algorithm 4 */

Algorithm 3: Voting Step

```
                                        /* Continuation of Voting Step */
25  foreach target l ← 1 to K do
26      for j ← 2 to v do
27          if j == 2 then
                if min(d_area(Pseg_{l,j}, Pseg_{1,j+1}), d_area(Pseg_{l,j},
28                  Pseg_{2,j+1}), ··· , d_area(Pseg_{l,j}, Pseg_{K,j+1})) == 0
                then
29                  Pseg_{l,j} ∈ epath_l;
30                  Pseg_{z_{j+1},j+1} ∈ epath_l;   /* Without loss of generality,
                    it is assumed that d_area(Pseg_{l,j}, Pseg_{z_{j+1},j+1}) = 0.  If
                    more than two segments have zero distance with
                    Pseg_{l,j}, the tiebreaker is the index x in Pseg_{x,j+1}.
                    */
31              else
32                  Pseg_{l,j} ∈ epath_l;
33              end
34          else
                if min(d_area(Pseg_{z_{j-1},j-1}, Pseg_{1,j}), d_area(Pseg_{z_{j-1},j-1},
35                  Pseg_{2,j}), ··· , d_area(Pseg_{z_{j-1},j-1}, Pseg_{K,j})) == 0
                then
36                  Pseg_{z_j,j} ∈ epath_l ;   /* Without loss of generality, it
                    is assumed that d_area(Pseg_{z_{j-1},j-1}, Pseg_{z_j,j}) = 0 */
37              end
38          end
39          if Pseg_{z_j,j} ∈ epath_l then
40              continue;
41          else
42              find the last determined segment in Pseg_{z_x,x} in epath_l;
                find min(d_area(Pseg_{z_x,x}, Pseg_{1,j}), d_area(Pseg_{z_x,x},
43                  Pseg_{2,j}), ··· , d_area(Pseg_{z_x,x}, Pseg_{K,j}));
                Pseg_{z_j,j} ∈ epath_l;   /* with out loss of generality, it is
                assumed that d_area(Pseg_{z_x,x}, Pseg_{z_j,j}) = 0   */
44          end
45      end
46  end
```

Algorithm 4: Voting Step (Continued from Algorithm 3)

CHAPTER VI

THEORETICAL ANALYSIS

In this Chapter, we analyze the effect of signal attenuation, the tracking resolution, and the effect of moving speed.

6.1 Signal Attenuation

Signal attenuation is a natural consequence of signal transmission over long distances. It is a function of transmission distance.

When static targets are being tracked, signal attenuation will not affect tracking performance. Since targets are static, the distance between targets and sensors does not change over time. So the attenuation can be modeled as a constant. For the same individual signal from a target, different sensors will observe different attenuation because of different transmission distance. So individual signals received by different sensors from the same target are different only by a scaling factor. The difference because of the scaling factor can be absorbed by the mixing matrix defined in the BSS model as Equation 4.1. So attenuation does not affect tracking static targets by our approach.

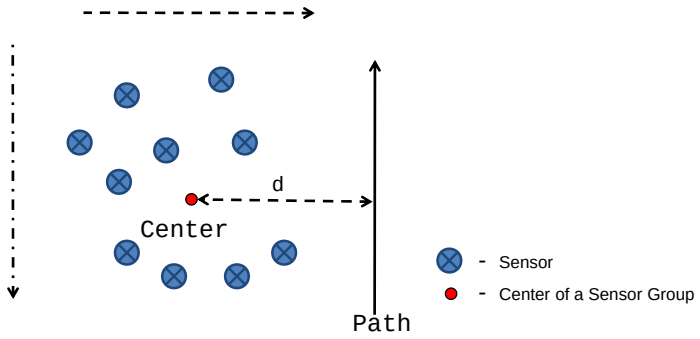

Figure 6: Setup for Experiments on Signal Attenuation. In the figure, the solid line and the dashed lines represent the moving paths taken by the target of interest and other targets respectively.

When moving targets are being tracked, signal attenuation may cause noise signals in the output of the separation step. When targets are moving, the difference between individual signals received by different sensors is not just a scaling factor. Because when a target is moving, the attenuation changes with the transmission distance between the target and a specific sensor. So the difference can not be absorbed by the mixing matrix. The consequences of the difference are: (a) Noise segments can be generated during separation because of the difference (b) Separated individual signals are less correlated with original individual signals. Clustering step, center selection step and voting step are designed with consideration of these consequences.

To show the effect of signal attenuation on the separation performance, we perform a simple experiment with moving targets. The experiment setup is as shown in Figure 6: Ten randomly placed sensors form a sensor group. Three targets are moving in the sensing range of the sensor group. We fixed the path of two targets (in dashed line) in our experiment and increase d the vertical distance between the center of the sensor group and the path taken by the target of interest. Figure 7 shows the maximum correlation between separated signals and the actual individual

signal from the target of interest. As we can observe that when the vertical distance increases, the correlation with original individual signal is higher. So the separation performance is better when the vertical distance increases. The reason is: When the vertical distance increases, the attenuation changes less. In turn, attenuated individual signals received by different sensors are less different from each other so that better separation performance can be achieved. From this experiment, we can also infer the effect of the sensor density. When more sensors are deployed in a field, it is more likely to have a sensor group both covering the path of interest and distant from the target at the same time. So a higher sensor density can lead to better separation performance.

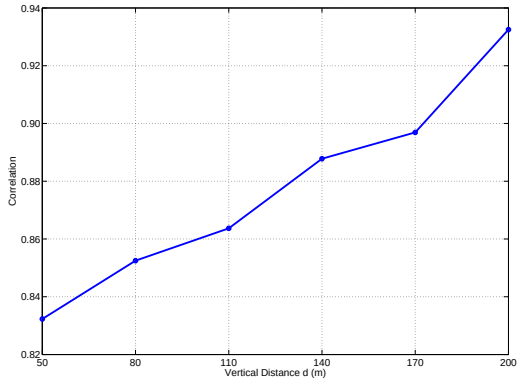

Figure 7: Effect of Attenuation

6.2 Tracking Resolution

We analyze the tracking resolution of the algorithm in this Chapter. The purpose of the analysis is to estimate achievable performance of the proposed tracking algorithm. We focus on the intersection step in the analysis.

First, we define *error distance* as follows:

Definition The error distance between a point in one intersection area and the path

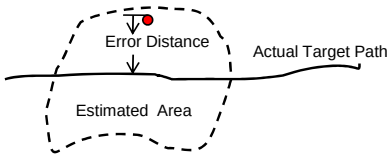

Figure 8: Error Distance. The area within the dashed line is the estimated area and the error distance between a dot within estimated area and the actual target path is shown in the figure.

of interest is the minimal distance between the point and any point on the path.

Mathematically, the error distance d_{err} between a point (x,y) in an estimated area A and an actual target path P is defined as follows:

$$d_{err}(x,y) = min_{(x_p,y_p)\in P}|(x,y) - (x_p,y_p)|_2 \quad , \tag{6.1}$$

where (x_p, y_p) represent a point on the actual target path P and $|\ |_2$ denotes the L_2-norm.

Tracking resolution is defined based on the error distance definition:

Definition Tracking resolution is defined as the average of error distance between all the points inside an intersection area and a path segment of interest.

Mathematically, the tracking resolution TR is defined as follows:

$$TR = \frac{\int_{(x,y)\in A} d_{err}(x,y)dxdy}{\int_{(x,y)\in A} dxdy} \quad . \tag{6.2}$$

As in Figure 8, error distance d_{err} is the minimum distance between the point inside estimated intersection area (represented with dot) and points on the path segment of interest. Tracking resolution is the average error distance of all the points inside an estimated intersection area.

We focus on linear path segments in theoretical analysis for the following reasons: (a) Any path can be formed with linear segments. (b) In practice the size of

signal segment used in the proposed algorithm is small so that estimated path segments are close to linear. To simplify the analysis of the tracking resolution we assume the path segment of interest fits inside the intersection area and it is perpendicular to the line joining centers of two sensor groups. We assume the sensors are uniformly distributed over the field. So sensor groups are also uniformly distributed over the field.

We assume N sensors are deployed in a field of size a meter by b meter and the sensing range of each sensor is R. Both the average tracking resolution and the finest tracking resolution are analyzed below.

6.2.1 Finest Tracking Resolution

The finest tracking resolution is defined as the achievable minimal mean error distance. We assume sensor groups are located within circles of radius r on average. So we have

$$\begin{aligned} \text{Sensor Density} &= \frac{N}{a \times b} \\ &= \frac{n_{group}}{\pi r^2} \end{aligned}$$

where n_{group} is the number of sensors in each sensor group. Thus the average radius r is

$$r = \sqrt{\frac{n_{group} ab}{\pi N}} \quad , \tag{6.3}$$

Theorem 6.2.1 *The finest tracking resolution of tracking a linear path segment of length l is* $\frac{(R+r)^2}{4l} sin^{-1}(\frac{l}{2(R+r)}) - \frac{1}{8}\sqrt{(R+r)^2 - (\frac{l}{2})^2}$.

The proof of Theorem 6.2.1 can be found in Appendix .1.

Corollary 6.2.2 *When the finest tracking resolution is achieved, the distance between the two neighboring sensor blocks is* $2\sqrt{(R+r)^2 - (\frac{l}{2})^2}$

Corollary 6.2.2 can be easily proven by extending Equation 1 in Theorem 6.2.1.

6.2.2 Average Tracking Resolution

The average tracking resolution predicts the average tracking accuracy achievable by the proposed tracking algorithm. It is the mean error distance averaged over all the possible cases.

Theorem 6.2.3 *The average tracking resolution of tracking a linear path segment of length* l *is* $\frac{(R+r)^2}{4l^2} sin^{-1}(\frac{l}{2(R+r)})((R+r) - 2\sqrt{(R+r)^2 - (\frac{l}{2})^2}) + \frac{3(R+r)^2}{16l} - \frac{l}{16}$.

The proof of Theorem 6.2.3 can be found in Appendix .2.

6.3 Effect of Moving Speed

In general, targets' moving speed affects performance of tracking algorithms. Tracking algorithms track moving targets by observing changes in sensing signals collected from sensors. If a target moves through a sensor-deployed field with very high speed, then sensors are not able to observe enough change in sensing signals for tracking. On the other hand, signals reported by sensors are digitized, i.e., sampled from original sensing signals. If a sensor can sample sensing signals with a high sampling rate, the sensing data collected from sensors can possibly capture enough changes for tracking fast-moving targets. To make moving speed discussed in this Thesis independent from the sampling rate, we use meter per sample interval as the unit for speed.

Low moving speed leads to better tracking performance. Since when a target is moving at low speed, more data samples can be collected from sensors. In the separation step, the separation performance for longer signal segments is generally better than the performance for shorter segments. So, in turn, better tracking performance can be achieved.

CHAPTER VII

EMPIRICAL EVALUATION

We evaluate the proposed tracking algorithm using data [32] collected from Mica2-compatible XSM motes, programmed using the nesC programming language and running the TinyOS operating system. The data was collected during simultaneous tracking of multiple targets as explained in [33].

Experimental set up is as shown in Figure 9(a). Five anchor nodes were placed at known positions, covering an area of approximately 27.4 meter by 27.4 meter. Four anchor nodes were placed in the corners of the square and the fifth anchor close to the center. The moving paths of targets are, a person holds two motes in two hands and walks on the rectangular track and another person holds single mote and walks on the triangular track. Sensors record the phase and frequency of an interference signals transmitted over 22 channels.

The signal strength of aggregate signals received by sensors can be calculated as follows:

$$\text{signal strength} \quad = \quad \sum_{i=1}^{22} \frac{distance}{att \times alpha} \quad , \tag{7.1}$$

where *att* is attenuation and *alpha* is attenuation coefficient calculated using fre-

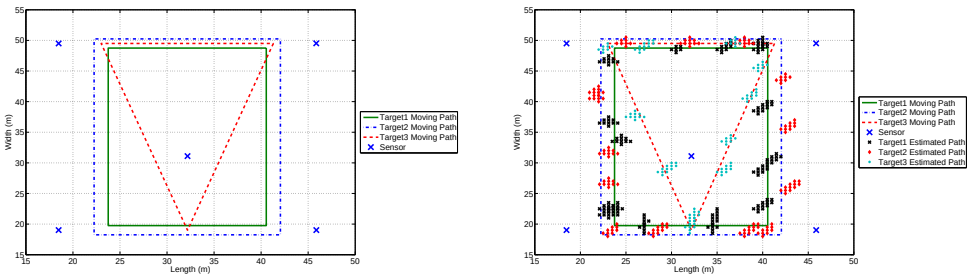

(a) Experimental Set UP (b) Our Tracking Result

Figure 9: Empirical Evaluation

quency from $[4, 30]$.

After calculating the aggregate signal strength values at each mote, we applied our tracking algorithm on signal strength data from sensors. Total data points used were 100 samples. We set the segment length to 50 samples and step size to 5 samples. The number of sensors per group are 3. To evaluate the performance according to intersection area, we quantize the whole field into 0.5 m by 0.5 m tiles. Tracking performance of our proposed algorithm is shown in Figure 9(b). Table I summarizes the comparison between the BSS-based approach and the radio interferometric approach [33]: The BSS-based approach can achieve comparable tracking performance.

Table I: Performance Comparison (NA- not Applicable)

Approach	Average of Error Distance (m)	Standard Deviation of Error Distance (m)
BSS-Based Tracking Algorithm	0.63	0.253
Radio Interferometric [33]	0.7	NA

Experiments in [33], estimate the moving track by collecting frequency and phase values. The hardware used in [33] is relatively sophisticated and costly because of frequency and data collection by motes. Our motes are required to collect only aggregate signal strength.

CHAPTER VIII

PERFORMANCE EVALUATION

We evaluate the performance of the proposed tracking algorithm with extensive simulations. We assume acoustic sensors are deployed in the field of interest for tracking purpose.

8.1 Experiment Setup

In the following experiments, the simulated field is a 1600m $\times$ 1600m square area. Sensors are randomly deployed in the field. The movement of targets is restricted to a 1000m $\times$ 1000m *center area* to eliminate boundary effects. The signals used for tracking are real bird signals downloaded from the website of Florida Museum of Natural History [21]. In our simulation experiments, we use FastICA [24] algorithm for signal separation. FastICA is an efficient and popular algorithm for independent component analysis in terms of accuracy and low computational complexity. The attenuation of sound signals is according to atmospheric sound absorption model [4,30]. The simulations are performed in Matlab. Following parameters are used in our experiments if not specified: (1) The sensing range of sensors is 250m. (2) Paths followed

by targets are generated randomly. (3) The number of sensors in each sensor group n_{group} is 10. (4) The number of moving targets in the field is 10. (5) Sensor density is sensors in the field. (6) The segment length is 100 samples and the step size is 10 samples. (7) Targets are moving at a speed below 0.15 meter per sample interval.

8.2 Performance Metrics

As described in Chapter 5.5 and 5.6, the estimated paths output by the target-tracking algorithm is essentially concatenated intersection areas. To evaluate the performance according to the concatenated intersection areas, we quantize the whole area using 5m $\times$ 5m tiles. One intersection area is represented by a set of points inside the area, each point representing the corner of the corresponding tile. Two metrics are used to evaluate the area: One is the *mean error distance*. It is based on the error distance defined in Chapter 6.2. The mean error distance is the mean of the error distance between all points inside concatenated intersection areas and the actual path taken by a target. The other is the *standard deviation of the error distance* between the points inside the concatenated intersection areas and the actual path taken by a target. The first one measures accuracy of the tracking algorithm and the second measures precision of the tracking algorithm. If we cast the evaluation of the estimation algorithm in terms of evaluating a statistical estimator, the accuracy corresponds to the bias of the estimator and the precision corresponds to the variance of the estimator.

The step size can affect both tracking performance and computational complexity. A big step size can reduce computation time with the cost of having gaps between concatenated intersection areas. We use *percentage of coverage* to measure the continuity in estimated paths. It is equal to one minus the ratio between the sum of distance between neighboring intersection areas and the length of the actual

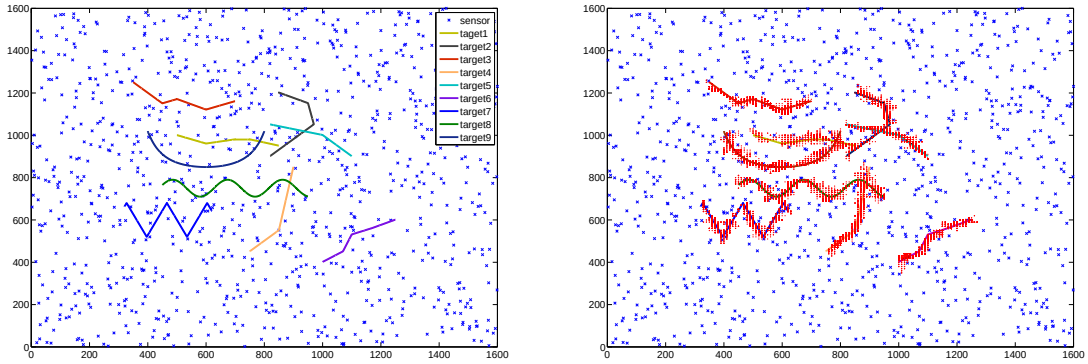

(a) Experiment Setup (b) Tracking Result

Figure 10: An Example

path. The distance between two intersection areas is defined as in Chapter 5.6: It is the distance between two closest points in each intersection area. If two intersection areas have overlap, the distance is zero.

8.3 A Typical Example

An example of typical results of the proposed tracking algorithm is shown in Figure 10. The paths taken by these targets are shown in Figure 10(a). The sensor density is 1000 sensors in the field. We include a zigzag[1] path in this example since the zigzag path is one kind of path with high frequency variation. Figure 10(b) shows paths estimated by our algorithm. The estimated paths are drawn in red dots. We can observe from the Figure 10 that the proposed tracking algorithm can track targets including targets following paths with high frequency variations, accurately and precisely.

[1]A formal definition of zigzag path is given in the Chapter 8.12 on experiments of paths with high frequency variation.

8.4 Effectiveness of BSS Algorithm

In this Chapter we investigate the relationship between the effectiveness of the BSS algorithms and tracking performance. In this set of experiments the number of moving targets is 10 and the sensor density is 1000 sensors in the field. Figure 11 show the relationship between separation performance and tracking performance. The X-axis is absolute value of correlation between center components selected in center selection step and original signals. A large value in X-axis indicates better separation performance. Y-axis is mean of error distance, measuring tracking performance. Figure 11 shows tracking performance increases with separation performance.

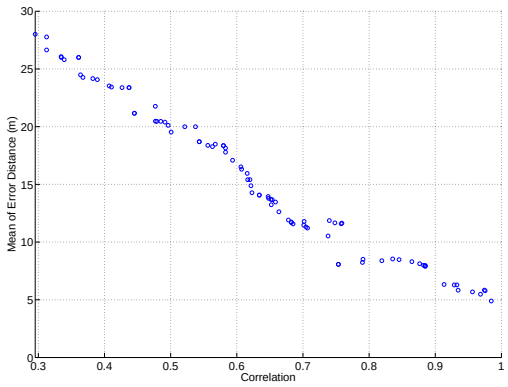

Figure 11: Effect of BSS Algorithm

8.5 Sensor Density vs Performance

As analyzed in Chapter 6, sensor density can greatly affect tracking performance. In this series of experiments, we increase the number of sensors in the field from 100 to 1000.

Figure 12(a) and 12(b) shows the tracking performance under different sensor densities. From Figure 12(a), we can observe: (a) The tracking algorithm can both

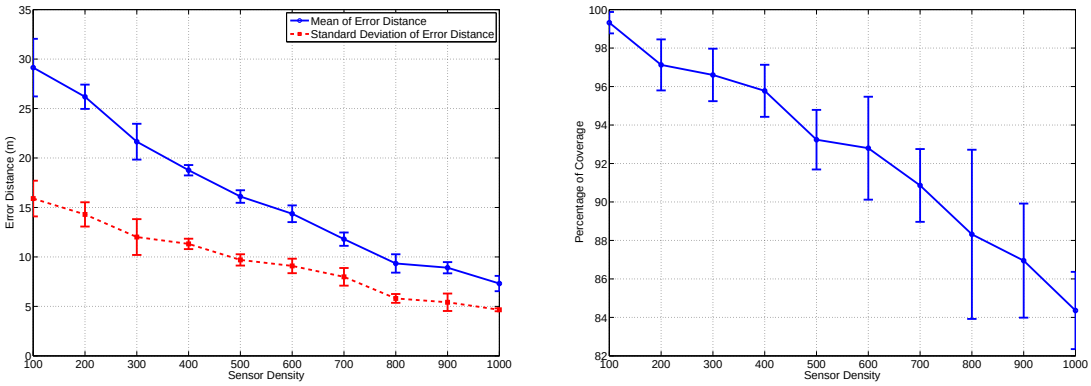

(a) Error Distance

(b) Percentage of Coverage

Figure 12: Tracking Performance for Different Sensor Density: with 95 Percent Confidence Interval

accurately and precisely track targets even when the sensor density is not high. (b) When the sensor density increases, the error distance decreases. This is because of two reasons: (a) When sensor density increases, more sensor groups can sense the target of interest. So intersecting sensing areas of more sensor groups can lead to smaller error distance. (b) When sensor density is high, better separation is possible as analyzed in Chapter 6.1. Figure 12(b) shows that percentage of coverage decreases when sensor density increases. In other words, when the sensor density increases, more gaps exist in the estimated paths. It is because of smaller or more precise intersection areas are estimated when sensor density increases. So the distance between two neighboring estimated path segments increases and more gaps are created in this way.

We compared theoretical results with experimental results in this set of experiments. The results are shown in Figure 13. For fair comparison, we fix targets' moving speed at 0.03 meter per sample in this set of experiments. We can observe the experimental curve is close to the theoretical curve of average tracking resolution. The experimental results are in the same order of the theoretical results. When the sensor density is larger than 1000, the difference between the two curves becomes

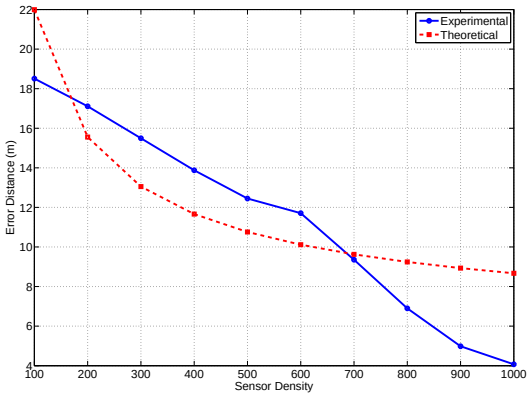

Figure 13: Comparison between Experimental Results and Theoretical Results

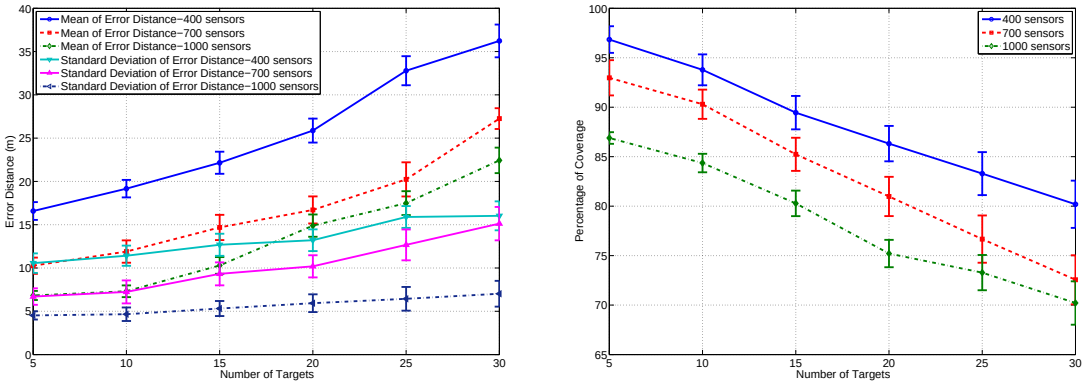

(a) Error Distance

(b) Percentage of Coverage

Figure 14: Tracking Performance for Different Number of Targets: with 95 Percent Confidence Interval

smaller because (1) Error distance decreases when sensor density increases for both curves. (2) The difference between these two curves is less than 9 meters when sensor density is larger than 1000.

8.6 Number of Targets

In this set of experiments, we vary the number of targets moving in the field. The results are shown in Figure 14. From Figure 14(a), we can observe: (a) When

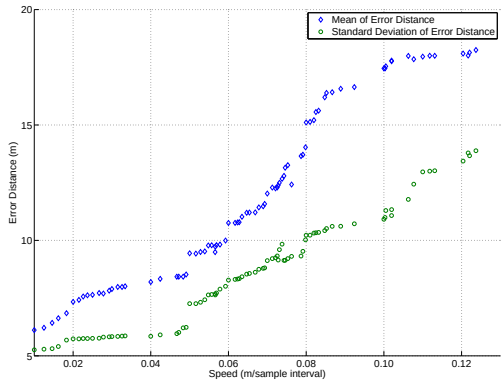

Figure 15: Scatter Plot of Tracking Performance vs. Moving Speed

the field is crowded with targets, our algorithm can still track targets with reasonable accuracy and precision. (b) The error distance increases when the number of targets increases. It is because the separation step can not perfectly separate out all the signals when the number of moving targets increases. As shown in Figure 14(b), the percentage of coverage decreases when the number of targets increases. The decrease is caused by the decrease in separation performance so that path segments estimated for different time slots are less consistently covering the actual paths.

8.7 Moving Speed

In this set of experiments, we investigate the effect of the moving speed on tracking performance. Targets in this set of experiments are moving with different speed. From experiment results shown in Figure 15, we can observe that the error distance increases when the moving speed increases. The reasons are as analyzed in Chapter 6.3: Speed increase can lead to decrease of separation performance and less number of sensor groups sense enough signal for tracking.

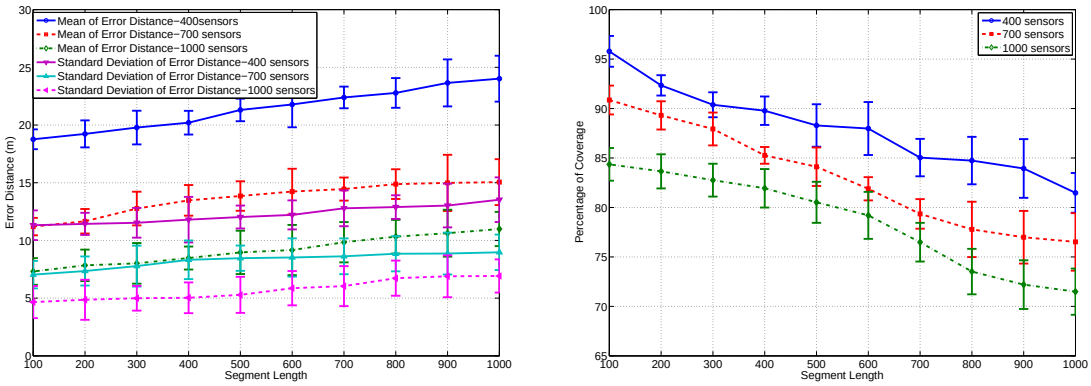

(a) Error Distance

(b) Percentage of Coverage

Figure 16: Effect of Signal Segment Length (l_{seg}) on Tracking Performance: with 95 Percent Confidence Interval

8.8 Segment Length (l_{seg})

This set of experiments focus on the length of signal segments used in tracking algorithm. In this set of experiments, we fix the step size at 10 samples and vary the segment length. Since the tracking algorithm processes signals in the unit of segments, the segment length is a critical parameter for the algorithm. The experiment results are shown in Figure 16. The results in Figure 16(a) indicate: The error distance increases when the segment length increases. It is because of less number of sensor groups which can "hear" targets for the whole path segment in their sensing ranges. The decrease in the number of sensor groups also causes the decrease in percentage of coverage as shown in Figure 16(b).

8.9 Step Size (l_{step})

In this set of experiments, we fix the segment length at 100 samples and vary the step size. As shown in Figure 17(a), the error distance increases with the step size.

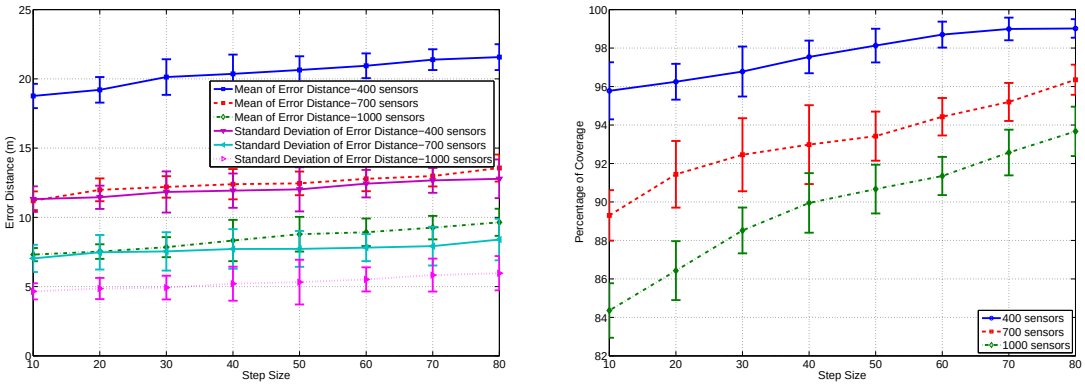

(a) Error Distance

(b) Percentage of Coverage

Figure 17: Effect of Step Size (l_{step}) on Tracking Performance: with 95 Percent Confidence Interval

This is because for a certain segment length, a larger step size reduces the length of common part of two successive time slots. In turn, the link correlation becomes less reliable. When the step size is comparable with the segment length, the percentage of coverage is high. It is because of larger intersection areas caused by less reliable link correlation.

8.10 Effect of Parameter n_{slot} in Center Selection Step

As described in Chapter 5.4, the parameter n_{slot} is used in the center selection step to select center segments. The parameter determines the number of successive time slots in consideration for picking center segments. We investigate the parameter with a set of experiments with different n_{slot}. The results are shown in Figure 18. From Figure 18(a), we can observe the drop in the error distance when n_{slot} is larger than one. It shows that increasing n_{slot} can significantly decrease the error distance by considering more successive time slots for picking center segments. The performance does not change significantly when n_{slot} is larger than four. We can also observe less percentage of coverage when n_{slot} is four in Figure 18(b). It is because the better

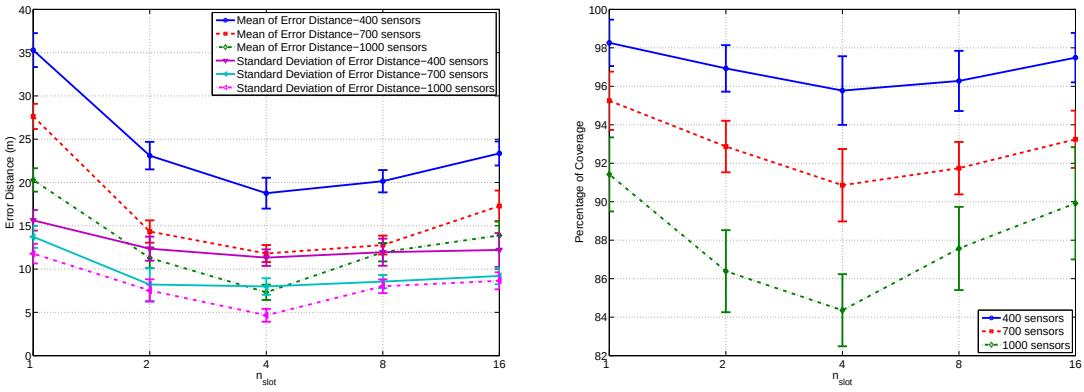

(a) Error Distance

(b) Percentage of Coverage

Figure 18: Effect of Parameter n_{slot} on Tracking Performance: with 95 Percent Confidence Interval

selection of center segments leads to more precise estimation of path segments and in turn these more precisely- estimated path segments can lead to more gaps in estimated paths.

8.11 Effect of Number of Sensors in Sensor Groups

In this Chapter, we describe our experiments on the parameter n_{group}, i.e., the number of sensors in each sensor group. The results are shown in Figure 19. As shown in the figure, the error distance is larger when n_{group} is too small or too large. When n_{group} is small, the number of targets can be larger than the number of sensors in a sensor group. Generally BSS algorithms perform better when the number of observations is larger than the number of individual signals. So more sensors in a sensor group can lead to better separation performance. But when the number of sensors in sensor group increases, the sensing range also increases. This lead to larger intersection areas when intersecting these larger sensing areas in the intersection step.

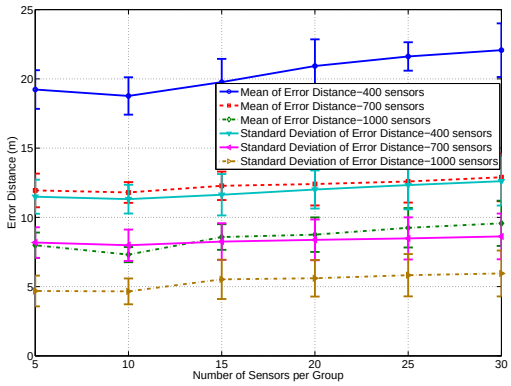

Figure 19: Effect of Number of Sensors in Sensor Groups: with 95 Percent Confidence Interval

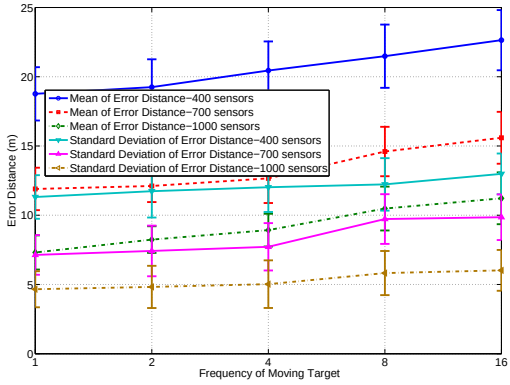

Figure 20: Path with High Frequency Variation: with 95 Percent Confidence Interval

8.12 Paths with High-Frequency Variations

In this set of experiments, we experiment on the performance of tracking targets following paths with high-frequency variations. In the experiments, we focus on paths between two points A and B with distance of 300m from each other as shown in Figure 21. Paths between these two points are zigzag paths of different periods. The width of the path is 100m and we vary zigzag period in our experiments. From the results shown Figure 20, we can observe the tracking algorithm can track targets following

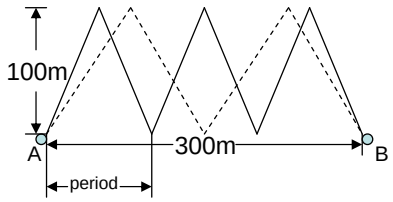

Figure 21: Example of Zigzag Path

zigzag paths accurately. We believe that the slight increase of error distance with the number of zigzag periods is because of higher speed required to finish longer paths. This experiments demonstrate the benefit of applying BSS algorithms in tracking targets. It enables tracking algorithms to have richer information for target-tracking. So the proposed algorithm can successfully track targets following paths with high-frequency variations.

CHAPTER IX

TOPOLOGIES OF SENSOR NETWORKS DEPLOYED FOR TRACKING

9.1 Introduction

In the previous chapters we focus on random topologies of high density sensor network. In the following chapters we focus on topologies of sensor network to improve tracking performance. The topology of a sensor network deployed for tracking is critical to tracking performance: (a) The topology affects separation performance. For better separation performance, sensors should be clustered so that there are more sensors than the number of targets within the sensing ranges of these sensors. It is because BSS algorithms perform better when the number of available mixtures are larger than the number of source signals. In general better separation performance leads to better tracking performance. (b) The number of sensors which can "hear" a target of interest determines how accurate and how precise a tracking algorithm can estimate the path taken by the target.

We propose cluster-based topologies for better tracking performance. Our contributions in this Thesis can be summarized as follows:

- We provide a list of necessary requirements on candidate topologies.
- We propose cluster-based topologies to improve tracking performance. Guidelines of parameter selection for proposed cluster topologies are given in the Thesis. We evaluate proposed topologies with extensive experiments.
- Our empirical experiments show that BSS-based tracking algorithms can achieve comparable performance in comparison with tracking algorithms assuming access to individual signals.
- We propose metrics to evaluate performance of proposed topologies using target-tracking algorithms. The metrics originate from the general metrics used to evaluate performance of an estimator in statistics since, essentially, target tracking algorithms *estimate* the paths based on data collected from sensor networks.

9.2 System Model and Goal

A general model of tracking targets using wireless sensor networks is shown in Figure 1.

The goal of this part of the Thesis is to improve tracking performance for tracking multiple targets with BSS algorithms. We use mean and standard deviation of error distance to measure tracking performance in this Thesis. The *error distance* is defined as the nearest distance between a specific point in the estimated areas to the actual path taken by a target as shown in Figure 8. The mean and standard deviation of error distance are calculated based on all the points in estimated areas. The mean and standard deviation of error distance measures the accuracy and precision of the tracking algorithm respectively. If we cast the evaluation of the estimation algorithm in terms of evaluating a statistical estimator, the accuracy corresponds to the bias of the estimator and the precision corresponds to the variance of the estimator.

9.3 Requirements on Candidate Topologies

We focus on topologies of *low-density* sensor networks simply because the effect of topologies on tracking performance is negligible for high-density sensor networks. In this Thesis, we assume that candidate topologies should satisfy the following requirements:

- Planned Deployment: The deployment used in tracking targets can be classified into two categories: random deployment [28] and planned deployment [22, 28]. In random deployment, sensors are distributed randomly over a field. We eliminate random deployment from consideration because for low-density sensor networks, the tracking performance of random deployment is usually worse than the tracking performance of planned deployment.

- Full Coverage: In planned deployment, we focus on topologies enabling sensors to cover the whole field of interest. This requirement is especially important for low-density sensor networks to prevent targets disappearing from tracking. One of the reasons to eliminate random deployment from consideration is because of its possibility of incomplete coverage for low-density sensor networks.

- Symmetrical Topology: In this Thesis we only consider symmetrical topologies. Symmetry is desired because targets can move in various directions and symmetrical topologies can ensure that tracking performance is direction-independent.

In this Thesis, we focus on topologies of sensor networks for BSS-based tracking algorithms: Blind source separation enables tracking algorithms to track multiple targets based on *individual signals* instead of *aggregate signals*. So BSS-based tracking algorithms can potentially track targets more accurately and precisely and they can track targets moving along paths of high-frequency variation. We introduce blind

source separation and rationale of applying blind source separation to the multiple target tracking problem below.

CHAPTER X

PROPOSED TOPOLOGIES OF WIRELESS SENSOR NETWORKS FOR TRACKING

In this Chapter, we introduce topologies proposed for BSS-based tracking algorithms. Before introducing the topologies, we first analyze separation performance in our experiments and describe rationale behind the proposed topologies.

10.1 Separation Performance

The key step in BSS-based tracking algorithms is to apply BSS algorithms to recover individual signals from aggregate signals so that tracking algorithms can have access to individual signals. Obviously the performance of separating out individual signals largely dictate overall tracking performance. To investigate the effect of topologies on separation performance, we did a series of initial experiments with random topologies.

In these initial experiments, 700 sensors are randomly distributed in a field of size $1.6km \times 1.6km$. To remove boundary issues, totally 15 targets are restricted to move in the field center of size $1km \times 1km$. Sensing range of each sensor is $250m$.

Table II: Separation Performance vs D_{center}

D_{center}(m)	P_{sep}
50 - 100	0.4841
100 - 150	0.5224
150 - 200	0.5301
200 - 250	0.5521
250 - 300	0.5132

Table III: Separation Performance vs D_{pair} $(200m < D_{center} < 250m)$

D_{pair}(m)	P_{sep}
50 - 70	0.681
70 - 90	0.6005
90 - 110	0.5152
110 - 130	0.4821

A correlation-based metric denoted by P_{sep} is used in our experiments to measure the separation performance. It is calculated by taking the absolute value of correlation between original signals and separated signals. We use absolute value because one separated signal may be of different sign in comparison with the corresponding original signal. The metric P_{sep} is within the range $[0, 1]$. Two topology-related metrics are used in our analysis. We represent the first metric as D_{pair}. It measures the average distance between each pair of sensors in a sensor group. The second metric measures the average distance between a target of interest and the center of the sensor group of interest when the target is moving. We represent the second metric as D_{center}. It is calculated by averaging over 100 data samples. Essentially, the metric D_{pair} measures clustering degree of neighboring sensors and the metric D_{center} measures the distance between a target and a cluster of sensors.

Figure 22 shows the separation performance of these initial experiments. We present the separation performance visually as a data image in Figure 22, the grid with the metrics D_{pair} and D_{center} on x-axis and y-axis respectively. The gray level of each pixel in the data image represents the separation performance P_{sep}: A darker pixel indicates better separation performance, i.e., a larger value of P_{sep}.

Table II summarizes separation performance in terms of the distance D_{center}. From Figure 22 and Table II, we can observe that the separation performance is best when the distance D_{center} is between 200m and 250m. In other words, the separation performance is best when the target is away from one sensor group and still within

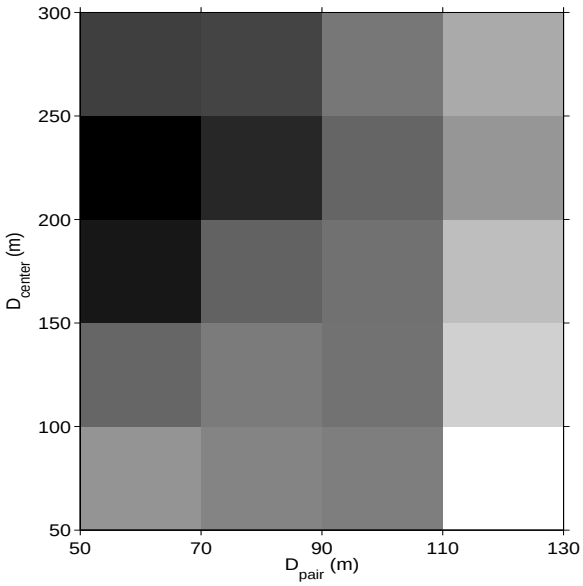

Figure 22: Effect of Topology on Separation

the sensing range of the sensor group.

Table III shows separation performance when D_{center} is between 200m and 250m. We can observe from Table III that the separation performance is better when D_{pair} is smaller. In other words, separation performance is better for sensor groups with sensors closer to each other, i.e., clustered together.

These two observations are because of signal attenuation, a natural consequence of signal transmission over long distances. Attenuation is a function of transmission distance. For static targets, attenuation does not affect separation performance since the distance between targets and sensors does not change over time. For a moving target, the distance between the target and sensors changes over time. So attenuation becomes, from a constant for static-target cases, into a function of time for moving-target cases. The attenuation functions for even two neighboring sensors are different. So two neighboring sensors in a sensor group may "hear" different signals from a target.

The difference causes noise in separation. Obviously, when sensors are closer

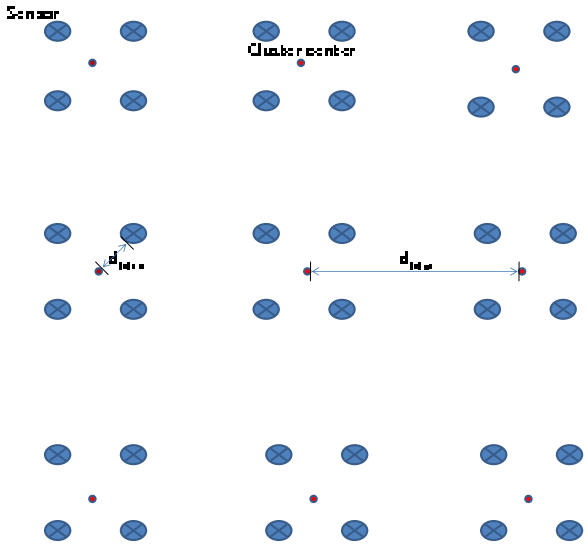

Figure 23: Example of Cluster Topology

to each other and the target of interest is away from these sensors, the difference in attenuation functions of these sensors is smaller. In turn, less noise is generated in separation and better separation performance can be achieved.

10.2 Proposed Topologies

Based on observations made in our initial experiments, we propose cluster topologies for BSS-based tracking algorithms as shown Figure 23:

In the proposed topologies, sensors are placed into clusters and sensor clusters are distributed evenly in a field. The proposed cluster topologies have four parameters:

- In-cluster arrangement: Within each cluster, sensors are arranged in regular patterns. The possible choices are any polygon-based patterns such as well-known triangle lattice pattern, square pattern, pentagon pattern, and hexagon pattern. Our experiments indicate that tracking performance is not sensitive to

patterns for in-cluster arrangement. So, we choose square pattern in this Thesis since research results on data segmentation [44], routing [19], and storage [10] recommend the square pattern. For the same reason, we arrange clusters in a field in square pattern.

- Number of sensors per cluster n_{clst}: This parameter specifies the number of sensors within each sensor cluster. For better separation performance, the number of sensors per cluster should be no less than the number of targets moving in the sensing range of a cluster. Potentially all the targets can move into the sensing range of one cluster, so we set the number of sensors per cluster close to the number of targets in the field.

- Inter-cluster distance d_{inter}: As shown in Figure 23, the inter-cluster distance is the distance between two centers of neighboring sensor clusters. This parameter depends on N, the total number of sensors to be deployed in the field, and n_{clst}, the number of sensors per cluster.

- Intra-cluster distance d_{intra}: Intra-cluster distance is the distance between the center of a sensor cluster and the furthest sensor within the same cluster. It is a measure of clustering degree. To avoid the merge of neighboring clusters, the parameter d_{intra} should be less than $\frac{d_{inter}}{2}$. Our initial experiments shown in Figure 22 indicate that better separation performance is achieved where sensors are close to each other. But it is not desired to cluster sensors in a very small area because (a) It may leave lots of uncovered spots in the field when sensor density is low. (b) When sensors are too close to each other, sensors "hear" roughly the same mixture of individual signals. In this case the separation performance can not be good. So we suggest d_{intra} to be close to $\frac{d_{inter}}{4}$. Our further experiments also support the choice of the parameter.

Besides considerations on separation performance, we propose cluster topologies because they satisfy the requirements listed in chapter 9.3: It is symmetric and it can cover the whole field. The proposed cluster topology is general: Grid topology is a special case of the cluster topology when $n_{clst} = 1$.

CHAPTER XI

PERFORMANCE EVALUATION OF PROPOSED TOPOLOGIES

We evaluate the performance of tracking algorithm in our proposed topology with extensive simulations with Matlab. We assume acoustic sensors are deployed in the field of interest for tracking purpose.

11.1 Experiment Setup

In the following experiments, the simulated field is a $1.6km \times 1.6km$ square area. The movement of targets is restricted to a $1km \times 1km$ *center area* to eliminate boundary effects. The signals used for tracking are real bird signals downloaded from the website of Florida Museum of Natural History [21]. The attenuation of sound signals is according to atmospheric sound absorption model [30]. We choose low-density sensor network with density N =128 and 288 sensors. The sensing range of sensors is 250m. In the following experiments, targets are moving at a speed below 0.15 meter per sample interval. The performance metrics used in our experiments is mean and standard deviation of error distance. In all the following experiments we compare our cluster topology with grid and random topologies.

11.2 Number of Sensors per Cluster (n_{clust})

In this set of experiments, we vary the number of sensors per cluster n_{clust}. We choose d_{intra}=80m according to parameter selection guidelines in chapter 10.2. The inter-cluster distance depends on the sensor density N and the number of sensors per cluster n_{clust}. For N=128, the inter-cluster distance d_{inter}=320m and 533.33m for n_{clust} =8 and 32 respectively. And for N=288, the inter-cluster distance d_{inter}=228.57m and 400m for n_{clust} =8 and 32 respectively. The number of moving targets $n_{targets}$ is 10 or 30 in this set of experiments. As shown in Figure 24, for the experiments on 128 sensors (N=128), the minimum error distance is achieved for 10 targets ($n_{targets}$=10) when n_{clust}=8. In the same experiments, the best tracking performance for 30 targets is achieved when n_{clust}=32. These experiment results indicate the number of sensors per cluster n_{clust} should be close to the number of targets as suggested in parameter selection guidelines given in Section 10.2. In comparison with grid and random topologies, performance increase for the cluster topology is 18.75% and 23.28% for 10 and 30 moving targets respectively when N=128. For 288 sensors (N=288), the increase is 26.12% and 27.90% for 10 and 30 moving targets respectively. We can also observe that performance of the cluster topology with selected parameters can be 33.62% and 32.78% better than random and grid topologies respectively.

11.3 Effect of In-Cluster Arrangement

In this set of experiments, we investigate the effect of in-cluster topologies. We experiment on the square pattern and the pentagon pattern as in-cluster arrangement. Similar experiment results are got from other polygons. Parameters used in this set of experiments are d_{intra}=80m and $n_{targets}$ =10. As shown in Figure 25(a) and 25(b), we observe that tracking performance is not sensitive to in-cluster arrangement.

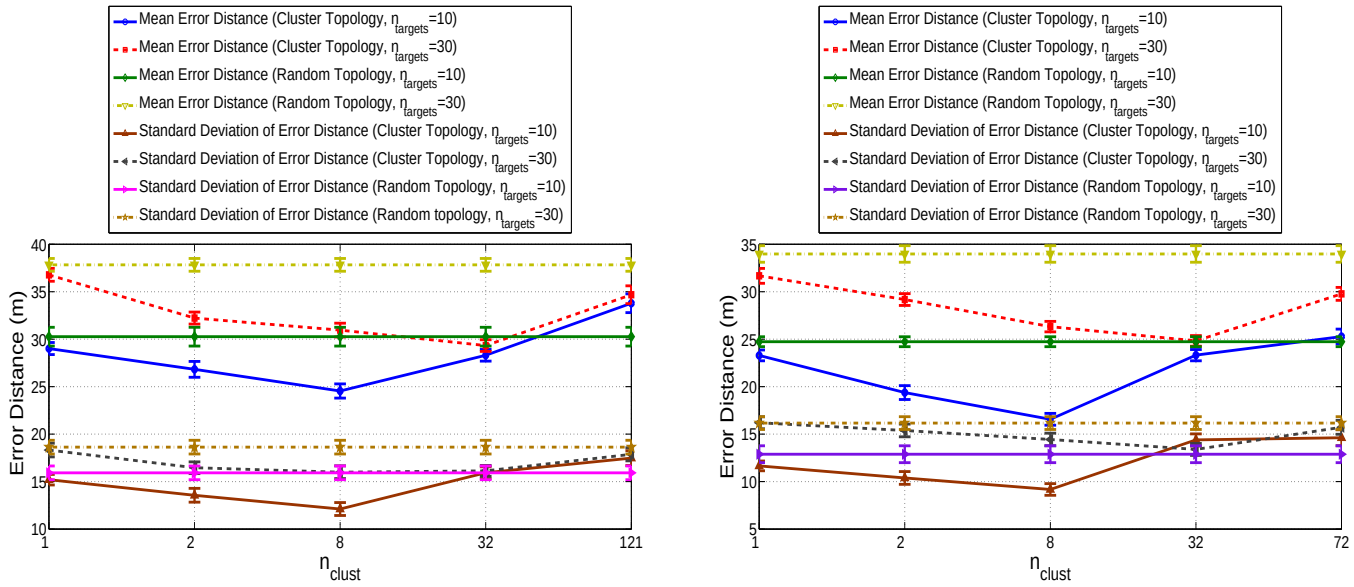

(a) N =128 (b) N =288

Figure 24: Effect of Number of Sensors per Cluster (n_{clust}) with 95 Percent Confidence Interval (When $n_{clust} = 1$, Cluster Topology essentially degenerates into Grid Topology.)

11.4 Effect of Intra-Cluster Distance (d_{intra})

In this set of experiments, we investigate the effect of d_{intra} on tracking performance. We choose n_{clust} to be 8 or 32 and vary d_{intra}. As shown in Figure 26(a), the best performance is achieved at d_{intra}=80m, i.e., $d_{intra} \approx \frac{d_{intra}}{4}$ as suggested in chapter 10.2. When intra-cluster distance is very small or even close to zero, sensors within a cluster observe signals from the same set of targets. So the aggregate signals received by the sensors within a cluster are close to each other. In turn, it degrades the separation performance. As shown in Figure 26(a), performance is getting better with the increase of d_{intra}. But when d_{intra} >80, error distance is increasing because the overlap of neighboring cluster's sensing ranges increases and bigger overlap area causes degradation in tracking performance.

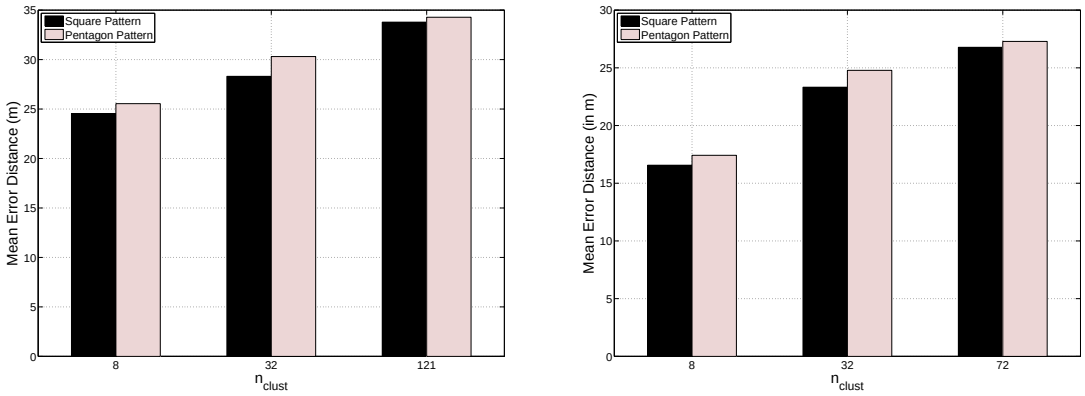

(a) Error Distance of N=128

(b) Error Distance of N=288

Figure 25: Effect of In-Cluster Arrangement on Tracking Performance

11.5 Effect of Number of Targets ($n_{targets}$)

In this set of experiments, we investigate the effect of number of targets on tracking performance. Table VII shows the typical performance increase of cluster topology over grid and random topologies. The experiment parameters are as follows: density N =288, n_{clust} =32, and d_{intra} =80m. Table IV, V, VI, VII shows percentage of increase in performance of cluster topology over grid and random topologies over different experiment settings. We can observe that percentage of increase can achieve 37.18% and 35.02% for 40 targets over random topologies and grid topologies respectively. Table VII shows that performance increase becomes larger when the number of targets increases. It is mainly because better separation performance can be achieved for cluster topology.

Table IV: Percentage increase in Performance of Cluster Topology Compared to Grid and Random Topologies (N =128, $n_{clust} = 8$)

$n_{targets}$	Performance Increase over Grid Topology	Performance Increase over Random Topology
5	17.23	22.59
10	18.75	23.28
15	19.54	23.64
20	20.57	23.94
25	21.12	25.55
30	22.77	26.65
35	24.37	27.48
40	26.65	29.88

Table V: Percentage increase in Performance of Cluster Topology Compared to Grid and Random Topologies (N =288, $n_{clust} = 8$)

$n_{targets}$	Performance Increase over Grid Topology	Performance Increase over Random Topology
5	24.21	25.47
10	26.12	27.90
15	28.16	29.77
20	29.52	29.86
25	30.07	30.08
30	32.66	33.02
35	33.67	34.44
40	34.87	36.53

Table VI: Percentage increase in Performance of Cluster Topology Compared to Grid and Random Topologies (N =128, $n_{clust} = 32$)

$n_{targets}$	Performance Increase over Grid Topology	Performance Increase over Random Topology
5	16.83	22.29
10	18.35	22.78
15	18.64	23.94
20	21.32	24.36
25	22.47	26.25
30	23.37	27.25
35	25.27	27.98
40	27.15	29.93

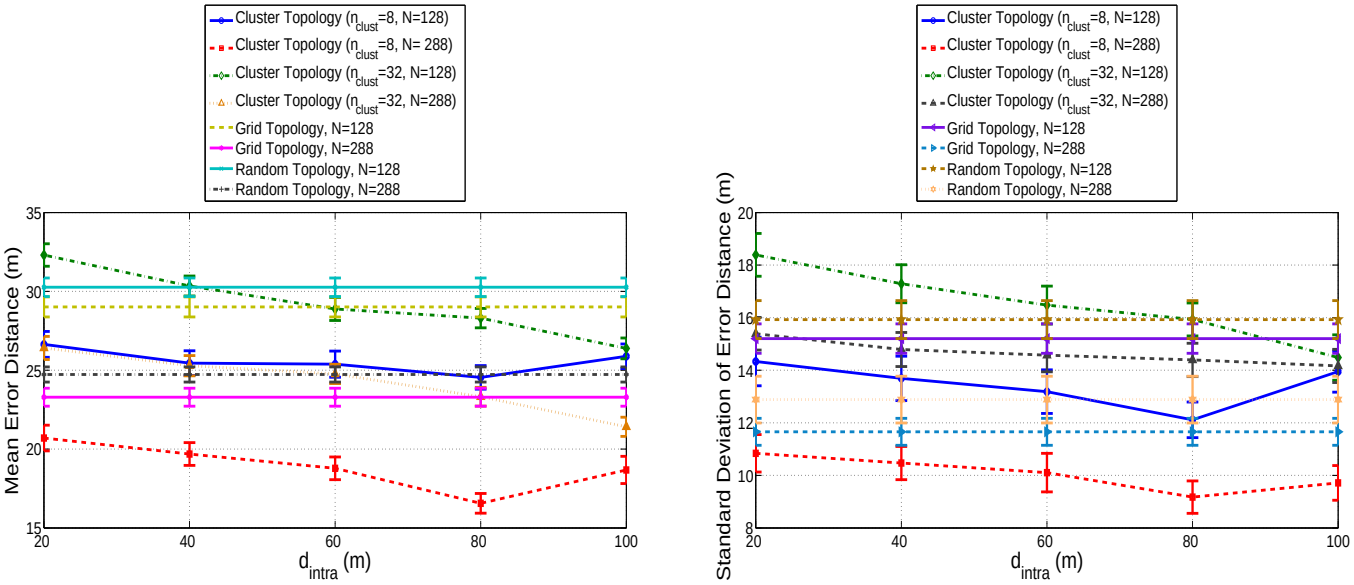

(a) Mean Error Distance

(b) Standard Deviation of Error Distance

Figure 26: Effect of Intra Cluster Distance (d_{intra}) on Tracking Performance with 95 Percent Confidence Interval

Table VII: Percentage increase in Performance of Cluster Topology Compared to Grid and Random Topologies (N =288, n_{clust} =32)

$n_{targets}$	Performance Increase over Grid Topology	Performance Increase over Random Topology
5	24.14	25.23
10	25.87	27.45
15	28.85	29.93
20	30.22	30.94
25	30.47	31.28
30	32.78	33.62
35	33.92	35.13
40	35.02	37.18

CHAPTER XII

DISCUSSION

The complexity of the algorithm is largely determined by the step size shown in Figure 3. The number of separations performed by the algorithm is in the order of $O(\frac{L}{l_{step}} \times N_{grps})$, where L is the total number of samples in one aggregate signal, l_{step} is the step size and N_{grps} is the number of sensor groups. A larger step size can reduce the number of separations performed by the algorithm. The cost will be slight degradation of tracking performance as shown in Figure 17(a).

In this Thesis, we assume the sensors are placed randomly in the field. From the analysis in Chapter 6, we know that better separation performance can be achieved when sensor groups are distant from targets and sense targets. So we can possibly reduce the number of sensors needed for tracking by placed sensors in a better way such as in clusters. This is one of the topics in our future work.

In this Thesis, we use BSS algorithms for the tracking purpose. The algorithms can also be used to process data collected by sensor networks for other applications. Since data collected by sensors is essentially aggregate data and BSS algorithms can recover data generated by different sources from aggregate data, analysis based on BSS algorithms can be more accurate.

CHAPTER XIII

CONCLUSION

We propose a general approach to track multiple targets using wireless sensor networks. The approach is based on blind source separation (BSS) algorithms. By applying BSS algorithms on aggregate signals collected from sensors, we can recover individual signals from targets for tracking. The proposed tracking algorithm fully utilize both spatial and temporal information available for tracking. We evaluate the proposed tracking algorithm both experimentally and theoretically. The tracking algorithm can track targets both accurately and precisely. Because of richer information made available by BSS algorithms, the proposed algorithm can also track paths with high-frequency variations. And also we propose cluster topologies to improve tracking performance of BSS-based tracking algorithms. A set of guidelines on parameter selection for proposed topologies are given in the Thesis. We evaluate proposed topologies with extensive experiments. The proposed topology can achieve more than 35 percent improvement in tracking performance over grid and random topologies. Our empirical experiments show that BSS-based tracking algorithm can achieve comparable tracking performance in comparison with algorithms assuming access to individual signals.

BIBLIOGRAPHY

[1] J. Aslam, Z. Butler, F. Constantin, V. Crespi, G. Cybenko, and D. Rus. Tracking a moving object with a binary sensor network. In *SenSys '03: Proceedings of the 1st international conference on Embedded networked sensor systems*, pages 150–161, New York, NY, USA, 2003. ACM.

[2] P. Bahl and V. N. Padmanabhan. RADAR: an in-building RF-based user location and tracking system. In *INFOCOM 2000. Nineteenth Annual Joint Conference of the IEEE Computer and Communications Societies. Proceedings. IEEE*, volume 2, pages 775–784, Tel Aviv, Israel, 2000.

[3] Y. Baryshnikov and R. Ghrist. Target enumeration via euler characteristic integrals. *SIAM J. Appl. Math*, 70(3):825–844, 2009.

[4] H. E. Bass, L. C. Sutherland, A. J. Zuckerwar, D. T. Blackstock, and D. M. Hester. Atmospheric absorption of sound: Further developments. *The Journal of the Acoustical Society of America*, 97(1):680–683, 1995.

[5] S. R. Blatt. Target Resolution in Distributed Sensor Systems. *NASA STI/Recon Technical Report N*, 3:15776–+, Oct. 2001.

[6] C. Savarese, J. Rabaey, K. Langendoen. Robust positioning algorithms for distributed ad-hoc wireless sensor networks. In *ATEC '02: Proceedings of the General Track of the annual conference on USENIX Annual Technical Conference*, pages 317–327, Berkeley, CA, USA, 2002. USENIX Association.

[7] J. Cardoso. Blind signal separation: statistical principles. *Proceedings of the IEEE*, 86(10):2009–2025, 1998.

[8] P. Comon. Independent component analysis, a new concept? *Signal Process.*, 36(3):287–314, 1994.

[9] K. Dantu, M. Rahimi, H. Shah, S. Babel, A. Dhariwal, and G. S. Sukhatme. Robomote: enabling mobility in sensor networks. In *IPSN '05: Proceedings of the 4th international symposium on Information processing in sensor networks*, page 55, Piscataway, NJ, USA, 2005. IEEE Press.

[10] G. Dimakis. Codes on graphs for distributed storage in wireless networks. *EECS Master Degree Thesis, University of California at Berkeley,http://www.eecs.berkeley.edu/adim/MS Thesis.pdf*, 2005.

[11] K. Doğançay and A. Hashemi-Sakhtsari. Target tracking by time difference of arrival using recursive smoothing. *Signal Process.*, 85(4):667–679, 2005.

[12] M. Drinic, D. Kirovski, and M. Potkonjak. Model-based compression in wireless ad hoc networks. In *SenSys '03: Proceedings of the 1st international conference on Embedded networked sensor systems*, pages 231–242, New York, NY, USA, 2003. ACM.

[13] R. O. Duda, P. E. Hart, and D. G. Stork. *Pattern classification, second edition.* Wiley, 2001.

[14] Edwards and R. G. Jayne. Location tracking using differential range measurements. volume 27, pages 199–205. ACTA PRESS, 2005.

[15] Q. Fang, F. Zhao, and L. Guibas. Lightweight sensing and communication protocols for target enumeration and aggregation. In *MobiHoc '03: Proceedings of the 4th ACM international symposium on Mobile ad hoc networking & computing*, pages 165–176, New York, NY, USA, 2003. ACM.

[16] D. S. Friedlander and S. Phoha. Semantic information fusion for coordinated signal processing in mobile sensor networks. *The International Journal of High Performance Computing Applications*, 2002.

[17] M. Gaeta and J.-L. Lacoume. Source separation without a priori knowledge: the maximum likelihood solution. In *Proc. EUSIPCO*, pages 621–624, Barcelona, Spain, 1990.

[18] S. Godsill and J. Vermaak. Variable rate particle filters for tracking applications. In *Statistical Signal Processing, 2005 IEEE/SP 13th Workshop on*, pages 1280–1285, July 2005.

[19] M. Goyeneche, J. Villadangos, J. J. Astrain, M. Prieto, and A. Cordoba. A distributed data gathering algorithm for wireless sensor networks with uniform architecture. In *PDP '07: Proceedings of the 15th Euromicro International Conference on Parallel, Distributed and Network-Based Processing*, pages 373–380, Washington, DC, USA, 2007. IEEE Computer Society.

[20] L. Gu, D. Jia, P. Vicaire, T. Yan, L. Luo, A. Tirumala, Q. Cao, T. He, J. A. Stankovic, T. Abdelzaher, and B. H. Krogh. Lightweight detection and classification for wireless sensor networks in realistic environments. In *SenSys '05: Proceedings of the 3rd international conference on Embedded networked sensor systems*, pages 205–217, New York, NY, USA, 2005. ACM.

[21] J. W. Hardy. Sounds of Florida's Birds, Florida Museum of Natural History, www.flmnh.ufl.edu/birds/sounds.htm, 1998.

[22] T. He, P. Vicaire, T. Yan, L. Luo, L. Gu, G. Zhou, R. Stoleru, Q. Cao, J. A. Stankovic, and T. Abdelzaher. Achieving real-time target tracking usingwireless sensor networks. In *RTAS '06: Proceedings of the 12th IEEE Real-Time and*

Embedded Technology and Applications Symposium, pages 37–48, Washington, DC, USA, 2006. IEEE Computer Society.

[23] Z. He, L. Yang, J. Liu, Z. Lu, C. He, and Y. Shi. Blind source separation using clustering-based multivariate density estimation algorithm. *Signal Processing, IEEE Transactions on [see also Acoustics, Speech, and Signal Processing, IEEE Transactions on]*, 48(2):575–579, Feb. 2000.

[24] C. W. Hesse and C. J. James. The fastica algorithm with spatial constraints. *Signal Processing Letters, IEEE*, 12(11):792–795, 2005.

[25] J. Hightower, C. Vakili, G. Borriello, and R. Want. Design and calibration of the spoton ad-hoc location sensing system, http://www.cs.washington. edu/homes/jeffro/pubs/hightower2001design/ hightower2001design.pdf, 2001.

[26] W. Hu, V. N. Tran, N. Bulusu, C. T. Chou, S. Jha, and A. Taylor. The design and evaluation of a hybrid sensor network for cane-toad monitoring. In *IPSN '05: Proceedings of the 4th international symposium on Information processing in sensor networks*, page 71, Piscataway, NJ, USA, 2005. IEEE Press.

[27] A. Hyvrinen and E. Oja. A fast fixed-point algorithm for independent component analysis. *Neural Computation*, 9:3917392–0, 1997.

[28] W. Kim, K. Mechitov, J.-Y. Choi, and S. Ham. On target tracking with binary proximity sensors. In *IPSN '05: Proceedings of the 4th international symposium on Information processing in sensor networks*, page 40, Piscataway, NJ, USA, 2005. IEEE Press.

[29] W. Kim, K. Mechitov, J.-Y. Choi, and S. Ham. target tracking with binary proximity sensors. *In Proc.IPSN,Los Angeles, California, USA*, April 2005.

[30] Kinsler, et al. In *Fundamentals of Acoustics*, New York, 2000. John Wiley Sons.

[31] C. Kreucher, K. Kastella, and I. Hero, A.O. Multitarget tracking using the joint multitarget probability density. *Aerospace and Electronic Systems, IEEE Transactions on*, 41(4):1396–1414, Oct. 2005.

[32] B. Kusy and J. Sallai. CRAWDAD data set vanderbilt/interferometric (v. 2007-06-06). Downloaded from http://crawdad.cs.dartmouth.edu/vanderbilt/interferometric, June 2007.

[33] B. Kusy, J. Sallai, G. Balogh, A. Ledeczi, V. Protopopescu, J. Tolliver, F. DeNap, and M. Parang. Radio interferometric tracking of mobile wireless nodes. In *MobiSys '07: Proceedings of the 5th international conference on Mobile systems, applications and services*, pages 139–151, New York, NY, USA, 2007. ACM.

[34] S.-P. K. Y.-C. T. F.-J. W. C.-Y. Lin. A probabilistic signal-strength-based evaluation methodology for sensor network deployment. *Advanced Information Networking and Applications, 2005. AINA 2005. 19th International Conference*, 1:Taipei, Taiwan, 319 – 324, March 2005.

[35] J. Liu, M. Chu, and J. Reich. Multitarget tracking in distributed sensor networks. *Signal Processing Magazine, IEEE*, 24(3):36–46, May 2007.

[36] R. F. Lutomirski and R. G. Buser. Phase difference and angle-of-arrival fluctuations in tracking a moving point source. *Appl. Opt.*, 13(12):2869, 1974.

[37] D. Macagnano, G. Destino, F. Esposito, and G. Abreu. Mac performances for localization and tracking in wireless sensor networks. In *Positioning, Navigation and Communication, 2007. WPNC apos;07.*, volume 22, pages 297 – 302, March 2007.

[38] B. Malhotra and A. Aravind. Path-adaptive on-site tracking in wireless sensor networks. *IEICE - Trans. Inf. Syst.*, E89-D(2):536–545, 2006.

[39] M. Moghavvemi and L. C. Seng. Pyroelectric infrared sensor for intruder detection. In *TENCON 2004. 2004 IEEE Region 10 Conference*, pages 656–659, Chiang Mai, Thailand, Nov. 2004.

[40] M. Morelande, C. Kreucher, and K. Kastella. A bayesian approach to multiple target detection and tracking. *Signal Processing, IEEE Transactions on*, 55(5):1589–1604, May 2007.

[41] A. Nasipuri and K. Li. A directionality based location discovery scheme for wireless sensor networks. In *WSNA '02: Proceedings of the 1st ACM international workshop on Wireless sensor networks and applications*, pages 105–111, New York, NY, USA, 2002. ACM.

[42] E. Olson, J. J. Leonard, and S. Teller. Robust range-only beacon localization. *Oceanic Engineering, IEEE Journal of*, 31(4):949–958, Oct. 2006.

[43] Q. Pan, J. Wei, H. Cao, N. Li, and H. Liu. Improved ds acoustic-seismic modality fusion for ground-moving target classification in wireless sensor networks. *Pattern Recogn. Lett.*, 28(16):2419–2426, 2007.

[44] A. Panangadan and G. Sukhatme. Data segmentation for region detection in a sensor network. *CRES Technical Report 05-005, University of Southern California,http://cres.usc.edu/cgi-bin/print pub details.pl?pubid=434*, 2005.

[45] A. Pereira, A. Monteiro, L. Nunes, and N. Costa. Wireless sensor network for mobile entities localization people monitor. In *ICSNC '07: Proceedings of the Second International Conference on Systems and Networks Communications*, page 51, Washington, DC, USA, 2007. IEEE Computer Society.

[46] D. Pham and P. Garrat. Blind separation of mixture of inde-

pendent sources through a quasi-maximum likelihood approach, citeseer.ist.psu.edu/pham97blind.html, 1997.

[47] K. Pister, J. Kahn, and B. Boser. Smartdust: wireless networks of millimeter-scale sensor nodes, 1999.

[48] N. B. Priyantha, A. Chakraborty, and H. Balakrishnan. The cricket location-support system. In *MobiCom '00: Proceedings of the 6th annual international conference on Mobile computing and networking*, pages 32–43, New York, NY, USA, 2000. ACM Press.

[49] S. Ray, W. Lai, and I. C. Paschalidis. Statistical location detection with sensor networks. *IEEE/ACM Trans. Netw.*, 14(SI):2670–2683, 2006.

[50] S. Ray, D. Starobinski, A. Trachtenberg, and R. Ungrangsi. Robust location detection with sensor networks. *IEEE Journal on Selected Areas in Communications*, 22(6):1016–1025, 2004.

[51] N. Shrivastava, R. M. U. Madhow, and S. Suri. Target tracking with binary proximity sensors: fundamental limits, minimal descriptions, and algorithms. In *SenSys '06: Proceedings of the 4th international conference on Embedded networked sensor systems*, pages 251–264, New York, NY, USA, 2006. ACM.

[52] J. Singh, U. Madhow, R. Kumar, S. Suri, and R. Cagley. Tracking multiple targets using binary proximity sensors. In *IPSN '07: Proceedings of the 6th international conference on Information processing in sensor networks*, pages 529–538, New York, NY, USA, 2007. ACM.

[53] L. D. Stone, T. L. Corwin, and C. A. Barlow. *Bayesian Multiple Target Tracking*. Artech House, Inc., Norwood, MA, USA, 1999.

[54] C. Tang and C. Raghavendra. Compression techniques for wireless sensor networks. pages 207–231. 2004.

[55] L. Tong, Y. Inouye, and R. Liu. Waveform-preserving blind estimation of multiple independent sources. *IEEE Transactions on Signal Processing*, 41(7):2461–2470, July 1993.

[56] L. Tong, V. Soon, and Y. F. H. R. Liu. Indeterminacy and identifiability of blind identification. *IEEE Transactions*, 38:499–509, March 1991.

[57] J. Vermaak, S. Godsill, and P. Perez. Monte carlo filtering for multi target tracking and data association. *Aerospace and Electronic Systems, IEEE Transactions on*, 41(1):309–332, Jan. 2005.

[58] B. Vo, N. Ma, P. Ching, and K. Wong. Tracking moving speech source using cyclic adaptive beamforming. *Electronics Letters*, 36(19):1666–1668, Sep 2000.

[59] P. von Rickenbach and R. Wattenhofer. Gathering correlated data in sensor networks. In *DIALM-POMC '04: Proceedings of the 2004 joint workshop on Foundations of mobile computing*, pages 60–66, New York, NY, USA, 2004. ACM.

[60] S. Yang, Y. Kim, and H. Choi. Vehicle identification using wireless sensor networks. In *Proceedings. IEEE, Richmond, VA,*, pages 41 – 46, March 2007.

[61] B. Zaidi, Z.R. Mark. A mobility tracking model for wireless ad hoc networks. In *Wireless Communications and Networking, 2003. WCNC 2003. 2003 IEEE*, volume 3, pages 1790– 1795, New Orleans, LA, USA, March 2003.

[62] G. V. Zàruba, M. Huber, F. A. Kamangar, and I. Chlamtac. Indoor location tracking using rssi readings from a single wi-fi access point. volume 13, pages 221–235, Hingham, MA, USA, 2007. Kluwer Academic Publishers.

APPENDIX

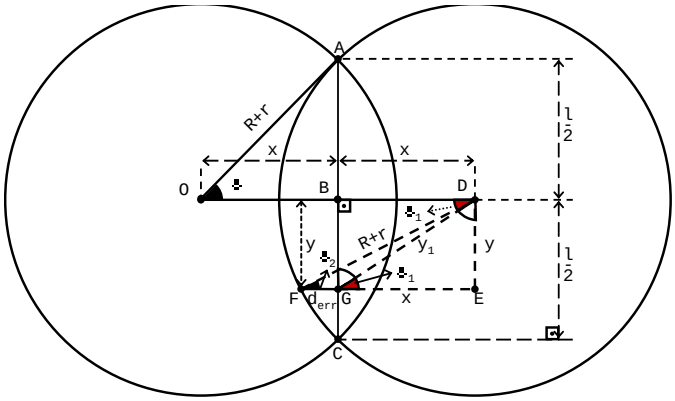

Figure 27: Finest Tracking Resolution

.1 Proof of Theorem 6.2.1

Proof The finest tracking resolution is achieved when the path segment of interest fits exactly into the intersection area of two sensing ranges as shown in Figure 27. It can be proven otherwise the tracking resolution becomes worse. In Figure 27, line segment AC is the linear path segment of length l. The corresponding estimated path segment covers the overlap of the two neighboring sensing ranges. So the path segment of interest is perpendicular to the line joining centers of sensor groups. The distance d_{err} is the distance between the sample point on the path denoted with G and the point on the perimeter of the sensing range denoted with F. Since d_{err} is the shortest distance from F to any points on the path segment, d_{err} is also the error distance between point F and the path segment. Suppose in Figure 27 the distance between centers of two neighbor sensor groups is $2x$. The value of x can be derived as follows. $\triangle OAB$ is a right angle triangle, $OA = R + r$ (the sensing radius of sensor group), and $AB = \frac{l}{2}$.

From $\triangle OAB$,

$$x = \sqrt{(R+r)^2 - (\frac{l}{2})^2} \quad . \tag{1}$$

Thus the distance between neighbor sensor groups is $2x$, i.e., $2\sqrt{(R+r)^2-(\frac{l}{2})^2}$. The error distance d_{err} can be derived as follows: From $\triangle DGE$ as shown in Figure 27,

$$\begin{aligned} tan\theta_1 &= \frac{y}{x} \ , \\ \theta_1 &= tan^{-1}\frac{y}{x} \ , \end{aligned} \tag{2}$$

$$x = \frac{y}{tan\theta_1} \ . \tag{3}$$

Now from $\triangle FDE$, $FD = R + r$ (the sensing radius of sensor group). We denote the distance between the point B and G with y. From $\triangle FDE$,

$$\theta_2 = sin^{-1}(\frac{y}{R+r}) \ , \tag{4}$$

and

$$\begin{aligned} tan\theta_2 &= \frac{y}{d_{err}+x} \ , \\ d_{err} &= \frac{y}{tan\theta_2} - x \ , \end{aligned} \tag{5}$$

where x is from Equation 3 and θ_2 is from Equation 4. Since

$$d_{err} = \frac{y}{tan\theta_2} - \frac{y}{tan\theta_1} \ , \tag{6}$$

we can further simplify the above equation by substituting θ_1 and θ_2 values derived in Equation 2 and Equation 4 respectively. So d_{err} can be derived as follows:

$$d_{err} = (R+r)\cos(\theta_2) - \sqrt{(R+r)^2-(\frac{l}{2})^2} \ . \tag{7}$$

For all the points on the line segment FG, the average error distance is $\frac{d_{err}}{2}$. Integral is used to calculate average of error distance for all the points within the intersection

area. Thus the finest tracking resolution is $\frac{1}{2}\int_0^{l/2}\{\frac{(R+r)cos(\theta_2)-\sqrt{(R+r)^2-(\frac{l}{2})^2}}{l}\}dy$ where $\theta_2 = sin^{-1}(\frac{y}{R+r})$.

After further simplification the finest tracking resolution becomes $\frac{(R+r)^2}{4l}sin^{-1}(\frac{l}{2(R+r)})-\frac{1}{8}\sqrt{(R+r)^2-(\frac{l}{2})^2}$.

.2 Proof of Theorem 6.2.3

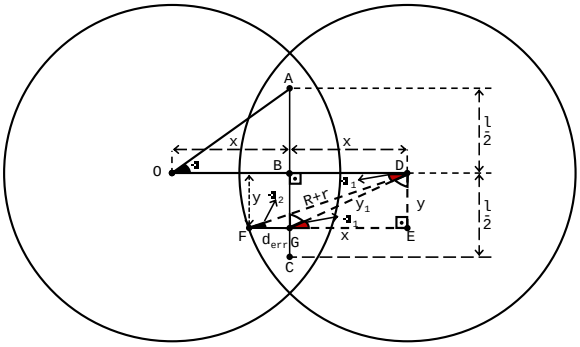

Figure 28: Average Tracking Resolution

Proof From $\triangle FDE$ as shown in Figure 28,

$$\begin{aligned} cos\theta_2 &= \frac{y}{R+r} \quad , \\ \theta_2 &= cos^{-1}(\frac{y}{R+r}) \quad . \end{aligned} \tag{8}$$

We derived the error distance d_{err} in Appendix .1.

$$d_{err} = \frac{y}{tan\theta_2} - \frac{y}{tan\theta_1} \quad , \tag{9}$$

we can further simplify the above Equation by substituting θ_1 and θ_2 values derived in Equation 2 and Equation 8 respectively. Then d_{err} can be derived as follows:

$$d_{err} = (R+r)\cos\theta_2 - x \quad , \tag{10}$$

where $\theta_2 = sin^{-1}(\frac{y}{r+R})$. So the mean error distance is $\frac{1}{2}\int_0^{l/2}\{(R+r)cos\theta_2 - x\}dy$.

From Corollary 6.2.2, we know the distance between the centers of two sensor groups when the finest tracking resolution is achieved. The worst-case tracking resolution is achieved when the distance between the centers of two sensor groups is

$R + r$. The average tracking resolution can be derived by integral of mean error distance over possible distance between the centers of two sensor groups. So the average tracking resolution is $\frac{1}{2} \int_{Z}^{R+r} \int_{0}^{\frac{l}{2}} \{\frac{(R+r)\cos\theta_2 - x}{l^2}\} dy dx$ where $Z = 2 \times \sqrt{(R+r)^2 - (\frac{l}{2})^2}$ and $\theta_2 = sin^{-1}(\frac{y}{r+R})$.

After further simplification the average tracking resolution is $\frac{(R+r)^2}{4l^2} sin^{-1}(\frac{l}{2(R+r)})((R+r) - 2\sqrt{(R+r)^2 - (\frac{l}{2})^2}) + \frac{3(R+r)^2}{16l} - \frac{l}{16}$.